

Performance Analysis Through Modeling & Simulation of Different Power Converters using MATLAB/Simulink

By

Md. Hasibul Bashar	142404
Khondokar Anwar Shadat	142418
Mecdad Marsad	142430

A Thesis Submitted to the Board of Examiners in Partial Fulfillment of the Requirement for the Degree of

**BACHELOR OF SCIENCE
IN
ELECTRICAL AND ELECTRONIC ENGINEERING**



Department of Electrical and Electronic Engineering
Islamic University of Technology
Board Bazar, Gazipur-1704, Bangladesh

November, 2018

Analysis of Overshoot Performance Through Modeling & Simulation of Different Power Converters using MATLAB/Simulink

Approved by:

Muhammad

Supervisor

Assistant Professor

Department of Electrical and Electronic Engineering,
Islamic University of Technology (IUT),
Boardbazar, Gazipur-1704.

Date:

Prof. Dr. Md. Ashraful Haque

Head of the Department

Department of Electrical and Electronic Engineering,
Islamic University of Technology (IUT),
Boardbazar, Gazipur-1704.

Date:

Table of Contents

List of Tables	5
List of Figures	6
List of Acronyms	8
Acknowledgements	9
Abstract	10
1 Introduction	11
1.1 DC-DC Converter	11
1.2 Review of DC-DC Converter	12
1.2.1 Review of DC-DC Converter according to Topology	12
1.2.2 Review of DC-DC Converter according to Application	14
1.2.3 Review of DC-DC Converter according to Control Strategy	15
1.3 Problem Identification and Research Motivation	18
1.4 Research Objective	19
1.5 Thesis Outline	19
2 Power Supply	20
2.1 Renewable Energy	20
2.2 Solar Energy	20
2.3 Distribution of Solar Radiation	21
2.4 Solar Radiation Reaching Earth Surface	22
2.5 Spectrum of Sun	23
2.6 Standard Test Conditions (STC)	24

3	Photovoltaic Cell	25
3.1	Definition	25
3.2	Photovoltaic Arrangements	25
3.2.1	Photovoltaic Cell	25
3.2.2	Photovoltaic Module	26
3.2.3	Photovoltaic Array	26
3.3	Material Used in PV Cell	27
3.4	Characteristics of PV Cell	28
3.4.1	Efficiency of PV Cell	29
3.5	Modelling of PV Array	30
3.5.1	PV Array Characteristics Curve	31
4	Converters	35
	DC-DC Converters	35
4.1	Buck Converter	36
4.1.1	Theory of Operation of Buck Converter	37
4.2	Boost Converter	41
4.2.1	Theory of Operation of Boost Converter	41

5	PID Integration	46
5.1	Fundamental operation of PID Controller	46
5.2	Ziegler Nicholes Method	49
5.3	Control System with PID Integration	51
5.3.1	Converters with PID Controller Integration	53
5.4	Percentage Overshoot	54
6	Result & Simulation	56
6.1.1	Parameter used for PV Array	56
6.1.2	PV Array Output	57
6.2.1	Parameter used for Converter and Controller	60
6.2.2	Converter Output	61
6.2.3	Converter Overshoot Comparison	63
7	Conclusion	64
	References	65
	Appendix	70

LIST OF TABLES

Table No.	Title	Page No.
5.1	Calculation of Ziegler Nichols Method	49
5.2	Effect of PID on Closed Loop System	50
6.1	PV Array Parameters for MATLAB Code	56
6.2	Converter and PID Controller Parameters for Simulink	60
6.3	Comparison Between Conventional and Proposed Buck Converter	63
6.4	Comparison Between Conventional and Proposed Boost Converter	63

LIST OF FIGURES

Figure No.	Title	Page No.
2.1	Solar Radiation and Distribution	21
2.2	Spectral radiation of Black body radiation and Sun Radiation	23
3.1	Basic Structure of PV Cell	25
3.2	Photovoltaic Cell	26
3.3	Equivalent circuit of a PV cell	28
3.4	Equivalent circuit of a PV cell	30
3.5	IV and PV Curve Characteristics	32
3.6	IV characteristics of Solar Array for fixed temperature but varying irradiance	33
3.7	PV characteristics of Solar Array for fixed irradiance but varying temperature	33
3.8	IV characteristics of Solar Array for fixed irradiance but varying temperature	34
3.9	PV characteristics of Solar Array for fixed irradiance but varying temperature	34
4.1	Block Diagram of DC-DC Converter	35
4.2	Buck Converter Circuit Diagram	36
4.3	The two circuit configurations of a buck converter: on-state, when the switch is closed; and off-state, when the switch is open (arrows indicate current according to the direction conventional current model).	37
4.4	Evolution of the voltages and currents with time in an ideal buck converter operating in continuous mode	39
4.5	Boost Converter Circuit Diagram	41

4.6	The two circuit configurations of a boost converter: on-state, when the switch is closed; and off-state, when the switch is open (arrows indicate current according to the direction conventional current model).	42
4.7	Evolution of the voltages and currents with time in an ideal boost converter operating in continuous mode	45
5.1	A block diagram of a PID controller in a feedback loop. $r(t)$ is the desired process value or setpoint (SP), and $y(t)$ is the measured process value (PV).	47
5.2	Simulink Diagram of Closed Loop Buck Converter with PID Controller.	53
5.3	Simulink Diagram of Closed Loop Boost Converter with PID Controller.	54
6.1	I-V Curve obtained for 28°C for various irradiance levels	57
6.2	P-V Curve obtained for 28°C for various irradiance levels	57
6.3	P-I curves obtained at 28°C for various irradiance levels	58
6.4	I-V curves obtained at an irradiance of 100 mW /cm ² for various temperatures	58
6.5	P-I curves obtained at an irradiance of 100 mW /cm ² for various temperatures	59
6.6	P-V curves obtained at an irradiance of 100 mW /cm ² various temperatures	59
6.7	Input-Output Curves of Buck converter with (i) conventional closed loop and (ii) proposed closed loop with PID	61
6.8	Input-Output Curves of Boost converter with (i) conventional closed loop and (ii) proposed closed loop with PID	62

LIST OF ACRONYMS

SMPS	Switch Mode Power Supply
IGBT	Insulated Gate Bipolar Transistor
PF	Power Factor
CCM	Continuous Conduction Mode
PWM	Pulse Width Modulation
RMS	Root Mean Square
f_s	Switching Frequency
D	Duty Cycle
T_{on}	Turn on Time
T_{off}	Turn off Time
LED	Light Emitting Diode
IC	Integrated Circuit
DSP	Digital Signal Processing
EMI	Electromagnetic Interference

ACKNOWLEDGEMENT

We have our sincerest appreciation for the help, assistance and advice that many people have given us on countless occasions during the course of our undergraduate work. First, we would like to express our profound gratitude to our supervisor for his guidance, support and encouragement. He has been a wonderful advisor, who has continuously inspired motivated us to complete many challenging research assignments. The other members of our thesis committee have given their thoughtful suggestions, and we would like to thank them all for that. Acknowledgement is due to EEE department of Islamic University of Technology for supporting our BSc thesis work.

We are very thankful to our family members for supporting us throughout our graduate study. Above all, we would like to glorify Almighty Allah Subhanahu Wa Ta'la for giving us knowledge and patience to carry out this work.

ABSTRACT

The recent upsurge in the demand of PV systems is due to the fact that they produce electric power without hampering the environment by directly converting the solar radiation into electric power. However, the solar radiation never remains constant. It keeps on varying throughout the day. The need of the hour is to deliver a constant voltage to the grid irrespective of the variation in temperatures and solar insolation. We have designed a circuit such that it delivers constant and stepped up dc voltage to the load. We have studied the closed loop characteristics of the PV array with variation in temperature and irradiation levels. Then we coupled the PV array with the boost converter in such a way that with variation in load, the varying input current and voltage to the converter follows the open circuit characteristic of the PV array closely. At various insolation levels, the load is varied and the corresponding variation in the input voltage and current to the boost converter is noted. It is noted that the changing input voltage and current follows the open circuit characteristics of the PV array closely. Initially three basic converters namely Buck, Boost and Buck-Boost were studied. Proper voltage regulation is obtained with the use of PID controller along with the converter. The proposed converters offered better efficiency, reduced overshoot. Converters offers best performances in simulation have been implemented in laboratory experiment. The input power of the converter is taken from the Photovoltaic cell which contains high distortion and harmonics. Moreover, it is a weak signal. For this step up, step down converters are used and with the integration of PID, better quality power supply can be ensured.

Chapter 1

Introduction

1.1 DC-DC Converter

A DC-to-DC converter is an electronic circuit or electromechanical device that converts a source of direct current (DC) from one voltage level to another. It is a type of electric power converter. Power levels range from very low (small batteries) to very high (high-voltage power transmission). DC to DC converters are commonly used as modern day power supplies. The converter builds the interface between utility power supply and electronic equipment connected to them. The process of rectification used to be simple, but recently, rectifiers have become much more sophisticated that, these are now systems rather than mere circuits [1] because of the requirement of quality power sources. Conventional DC to DC converters in bridge configuration suffer from the problems of low conversion efficiency at extremely low duty cycles with the addition burden of distorted input current at low power factor [1]-[3], The distorted non-sinusoidal current is because of the fact that, these converters draw current from the DC line only if DC link voltage is lower than the rectified line voltage. To minimize the harmonic distortions caused by DC to DC converters, various methods have been developed and proposed. The use of input filter is a simple way to address the problem, but the size of the inductor and capacitor required in filter design are large.

Generally, to sort out the problem, two power-processing stages are employed. Improved power factor along with a constant DC link voltage is provided by the input PFC stage. Conventional PFC stage employs a Boost converter [11]-[13]. DC to DC converter in output stage chops the output current/voltage at high frequency [14], this is being reflected at the source side in the form of chopped high frequency DC input current [15]. Therefore, a small filter to keep the sinusoidal shape of the input current at high power factor is used. Such result is possible only with full wave pulsed DC output. A constant DC voltage with low ripple is considered as quality DC power supply. Generally, large capacitor is used as

output filter to keep the output voltage constant. For boost conversion, unidirectional switch used in DC to DC converter stage has to operate in critical conduction mode [16]-[19] in other words, switching of the power (i.e. Turn ON) should be done at the instant of zero current crossing of the boost diode. To ensure critical conduction mode with changes either in load or the input voltage, adjustable switching frequency has to be applied to DC to DC converter.

In this paper, buck, boost and buck-boost converters are compared and better performing converters are designed from it using PID controllers to obtain high conversion efficiency at extremely low conditions. High input power factor is ensured with suitable feedback control is kept within the tolerable limits specified by IEEE-519.

1.2 Review of DC-DC Converter

The reported works in AC-DC conversion can be reviewed in accordance to their topologies, applications and control strategies.

1.2.1 Review of DC-DC Converter according to Topology

Practical electronic converters use switching techniques. Switched-mode DC-to-DC converters convert one DC voltage level to another, which may be higher or lower, by storing the input energy temporarily and then releasing that energy to the output at a different voltage. The storage may be in either magnetic field storage component (inductors, transformers) or electric field storage components (capacitors). This conversion method can increase or decrease voltage. Switching conversion is more power efficient (often 75% to 98%) than linear voltage regulation, which dissipates unwanted power as heat. Fast semiconductor device rise and fall times are required for efficiency; however, these fast transitions combine with layout parasitic effects to make circuit design challenging. The higher efficiency of a switched-mode converter reduces the heatsinking needed, and increases battery endurance of portable equipment. An important improvement in DC-DC converters is replacing the flywheel diode by synchronous rectification [6],

whose "on resistance" is much lower, reducing switching losses. Before the wide availability of power semiconductors, low-power DC-to-DC synchronous converters consisted of an electro-mechanical vibrator followed by a voltage step-up transformer feeding a vacuum tube or semiconductor rectifier, or synchronous rectifier contacts on the vibrator.

Most DC-to-DC converters are designed to move power in only one direction, from dedicated input to output. However, all switching regulator topologies can be made bidirectional and able to move power in either direction by replacing all diodes with independently controlled active rectification. A bidirectional converter is useful, for example, in applications requiring regenerative braking of vehicles, where power is supplied *to* the wheels while driving, but supplied by the wheels when braking.

Although they require few components, switching converters are electronically complex. Like all high-frequency circuits, their components must be carefully specified and physically arranged to achieve stable operation and to keep switching noise (EMI / RFI) at acceptable levels. Their cost is higher than linear regulators in voltage-dropping applications, but their cost has been decreasing with advances in chip design.

DC-to-DC converters are available as integrated circuits (ICs) requiring few additional components. Converters are also available as complete hybrid circuit modules, ready for use within an electronic assembly.

Linear regulators which are used to output a stable DC independent of input voltage and output load from a higher but less stable input by dissipating excess volt-amperes as heat, could be described literally as DC-to-DC converters, but this is not usual usage. (The same could be said of a simple voltage dropper resistor, whether or not stabilized by a following voltage regulator or Zener diode.)

There are also simple capacitive voltage doubler and Dickson multiplier circuits using diodes and capacitors to multiply a DC voltage by an integer value, typically delivering only a small current.

1.2.2 Review of DC-DC Converter according to Application

DC to DC converters are used in portable electronic devices such as cellular phones and laptop computers, which are supplied with power from batteries primarily. Such electronic devices often contain several sub-circuits, each with its own voltage level requirement different from that supplied by the battery or an external supply (sometimes higher or lower than the supply voltage). Additionally, the battery voltage declines as its stored energy is drained. Switched DC to DC converters offer a method to increase voltage from a partially lowered battery voltage thereby saving space instead of using multiple batteries to accomplish the same thing.

Most DC to DC converter circuits also regulate the output voltage. Some exceptions include high-efficiency LED power sources, which are a kind of DC to DC converter that regulates the current through the LEDs, and simple charge pumps which double or triple the output voltage.

DC to DC converters developed to maximize the energy harvest for photovoltaic systems and for wind turbines are called power optimizers.

Transformers used for voltage conversion at mains frequencies of 50–60 Hz must be large and heavy for powers exceeding a few watts. This makes them expensive, and they are subject to energy losses in their windings and due to eddy currents in their cores. DC-to-DC techniques that use transformers or inductors work at much higher frequencies, requiring only much smaller, lighter, and cheaper wound components. Consequently, these techniques are used even where a mains transformer could be used; for example, for domestic electronic appliances it is preferable to rectify mains voltage to DC, use switch-mode techniques to convert it to high-frequency AC at the desired voltage, then, usually, rectify to DC. The entire complex circuit is cheaper and more efficient than a simple mains transformer circuit of the same output.

1.2.3 Review of DC-DC Converter according to Control Strategies

The primary control objective of the DC-DC converter is to regulate the output voltage. The feedback controller to regulate the output voltage must be designed with the following objectives in mind: zero steady state error, fast response to changes in the input voltages and the output load, low overshoot, and low noise susceptibility. The performance of the converter system largely depends on the quality of the applied current control strategy to achieve high efficiency, low percentage overshoot almost sinusoidal input current and high input power factor.

Linear and Non-linear Control

The linear controller operates with conventional voltage type PWM modulators. In contrast to the nonlinear controllers, linear controller schemes have separated current error compensation and voltage modulation parts. This concept allows exploiting the advantages of open-loop modulators (sinusoidal PWM, space-vector modulator, and optimal PWM) which are of constant switching frequency type. In the linear group, some basic controllers are reported: PI stationary and synchronous, state feedback, and predictive with constant switching frequency. Besides linear control, non-linear control like hard switch converter, Neural Network (NN) controller, FLCC controllers are also reported in literature for the control of static power converters.

Current Mode Control Techniques

The research in sensor less control has resulted in Direct Power Control and Voltage Oriented Control in the past. One cycle controlled system has been reported as another sensorless strategy which does not require AC voltage sensors and phase locked loop (PLL) for synchronization. Reference proposes to eliminate the voltage sensors that are required for stable operation of OCC based bidirectional three phase DC-DC converter. The indirect current control is one of the earliest applications which eliminate current transducers in controlling input current of PWM rectifiers, where, the current control strategy is based on

a complete dynamical model of the converter resulting linear system of second order, compared with the fourth-order system in the previous ones. This simplifies the stability analysis and greatly facilitates the design of the PI voltage regulator.

Direct Current Control Techniques

Average Current Mode Control (ACMC)

In order to follow the reference with as little overshoot as possible, an average-current mode control is used with a high bandwidth, where the error between the reference inductor current and measured inductor current is amplified by a current controller to produce the control voltage. The control voltage is compared with a ramp in the PWM controller to produce the switching signal.

Hysteresis Current Mode Control (HCMC)

In HCMC, inductor current is kept in between the two sinusoidal current references generated corresponding to maximum and minimum boundary limits. To keep the current sinusoidal as possible or to achieve smaller ripple in the input current, a narrow hysteresis band is desired. The narrower the hysteresis band, the higher is the switching frequency. According to this control technique, the switch is turned ON when the inductor current decreases below the lower reference and is turned OFF when the inductor current increases above the upper reference, giving rise to a variable frequency control.

Predictive Current Mode Control (PCMC)

In predictive current control scheme the switch voltage is predicted at the beginning of each modulation/ switching period. The prediction is based on the current error, input voltage, switching frequency and input filter inductor and load variables. The predicted switch voltage is compared with double-edge triangular carrier signal to generate PWM pulse to the switches. The carrier signal is chosen for fixed frequency operation but the amplitude of the carrier signal is modulated to accommodate the load voltage/current

variation. In every switching/modulation cycle, the switch voltage reference is predicted and used to generate gate pulses. This technique uses additional information along with error signal that improves converter dynamic performance. The improvements occur at the expense cost on sensors and complexity in control circuits.

Linear Current Control (LCC)

In LCC the actual current is compared to the reference current to obtain the current error. The error is processed by a proportional-integral controller to provide a modulating signal for a PWM modulator. The modulator produces gate pulses for the converter switches. The pulses are of constant frequency with varying pulse widths, which depends on the magnitude of the modulating signals produced by the current controller. The controller parameters are tuned to optimize the PWM pulses such that the input current maintains near sinusoidal waveform and the power factor near to unity. The controller requires minimum number of measured signals from converter and hence the implementation using standard integrated circuits becomes simple, cost-effective and reliable. In a rectifier current regulation scheme is presented that relies on calculation of duty cycle for each switching state (space vector) of the rectifier. This fundamental concept is extended to a deadbeat, predictive, rectifier current regulator. Direct control of current space (d_q) vectors has the advantages of improved harmonic performance, especially at low dc bus voltages (modulation index near unity), and improving dynamic response to a transient in the load power or dc bus voltage at any operating condition in comparison to per-phase PWM techniques.

Nonlinear Carrier Control (NLC)

The NLC is capable of attaining input resistor emulation in boost and other converters that operate in the continuous conduction mode. Implementation of the controller is quite simple, with no need for sensing of the input voltage or input current. There is also no need for a current loop error amplifier. The boost nonlinear-carrier charge controller is

inherently stable and is free from the stability problems that require addition of an artificial ramp in current programmed controllers [1].

Other Control Techniques

Apart from the discussed control techniques, there are lot of other control techniques like digital boundary current control, sliding mode control, Lyapunov based control, direct power control, inductor voltage control and digital control.

1.3 Problem Identification and Research Motivation

Power quality issue is becoming important in areas involving use of power electronic control of DC-DC converters. Research continues to improve the power quality in all fields of electricity use. DC-DC converters with improved power quality are complex, costly, difficult to maintain and unreliable in some cases. Present research work will emphasize to simplify the circuit topology and make cost effective solutions of power quality issues of single phase DC-DC converters. Previous works concentrated on two stage solution consists of diode bridge rectifiers followed by conventional DC-DC converters. One stage solutions by single phase DC-DC conversion will necessitate new single phase topologies. The implementation of new single phase DC-DC conversion including PID controller will ensure better and reliable DC output to the load. The input current will then be filtered and controlled by average current control technique to obtain near sinusoidal current with good converter efficiency and high input power factor. The new single phase AC to DC converter topologies will be investigated by simulation. It is anticipated that innovations and ideas generated during this research will be of significant contribution to the power quality mitigation of single phase DC-DC conversion.

1.4 Research Objective

To overcome the problems experienced in switch mode DC-DC converter, the objective of this thesis research is to propose new and simple easy to control topologies to maintain low percentage of overshoot. Thus the objectives are:

- 1) To achieve high efficiency at extremely low and high duty cycle of the switching frequency using hybrid diode-capacitor network instead of conventional transformers for voltage step-down operation.
- 2) Developing small signal model of the converter to design suitable feedback control to regulate the percentage overshoot of the output voltage.
- 3) The converter must maintain constant output voltage under load variation. The dynamic response validated that.

1.5 Thesis Outline

Chapter 1 provides the instruction and literature review regarding DC-DC converter, research motivation etc.

Chapter 2 provides a detailed outline regarding renewable energy, mostly solar energy.

Chapter 3 provides a detailed description of the making, equation and the mechanism of Photovoltaic Cell.

Chapter 4 provides knowledge on the converters namely buck & boost converter.

Chapter 5 illustrates the basics and uses of PID controller, its mechanism and finally the use of PID controller as a closed loop feedback of the basic buck and boost converters.

Chapter 6 shows the used parameters of the PV cell, the converters and the PID controller along with the performance analysis of the converters among their open loop and closed loop systems.

Chapter 7 draws a conclusion of the current work.

Chapter 2

Power Supply

The input power of the converter is taken from renewable energy sources. In this thesis work, solar energy is utilized through Photovoltaic cell and the output voltage and current is taken from the Photovoltaic cell to the converter input.

2.1 Renewable Energy

Renewable energy sources also called non-conventional type of energy are the sources which are continuously replenished by natural processes. Such as, solar energy, bio-energy - bio-fuels grown sustainably, wind energy and hydropower etc., are some of the examples of renewable energy sources. A renewable energy system convert the energy found in sunlight, falling-water, wind, sea-waves, geothermal heat, or biomass into a form, which we can use in the form of heat or electricity. The majority of the renewable energy comes either directly or indirectly from sun and wind and can never be fatigued, and therefore they are called renewable [12].

However, the majority of the world's energy sources came from conventional sources-fossil fuels such as coal, natural gases and oil. These fuels are often term non-renewable energy sources. Though, the available amount of these fuels are extremely large, but due to decrease in level of fossil fuel and oil level day by day after a few years it will end. Hence renewable energy source demand increases as it is environmental friendly and pollution free which reduces the greenhouse effect [12].

2.2 Solar Energy

Solar energy is a non-conventional type of energy. Solar energy has been harnessed by humans since ancient times using a variety of technologies. Solar radiation, along with secondary solar-powered resources such as wave and wind power, hydroelectricity and

biomass, account for most of the available non-conventional type of energy on earth. Only a small fraction of the available solar energy is used [13].

Solar powered electrical generation relies on photovoltaic system and heat engines. Solar energy's uses are limited only by human creativity. To harvest the solar energy, the most common way is to use photo voltaic panels which will receive photon energy from sun and convert to electrical energy. Solar technologies are broadly classified as either passive solar or active solar depending on the way they detain, convert and distribute solar energy.

Active solar techniques include the use of PV panels and solar thermal collectors to strap up the energy. Passive solar techniques include orienting a building to the Sun, selecting materials with favorable thermal mass or light dispersing properties and design spaces that naturally circulate air [5]. Solar energy has a vast area of application such as electricity generation for distribution, heating water, lightening building, crop drying etc.

2.3 Distribution of Solar Radiation

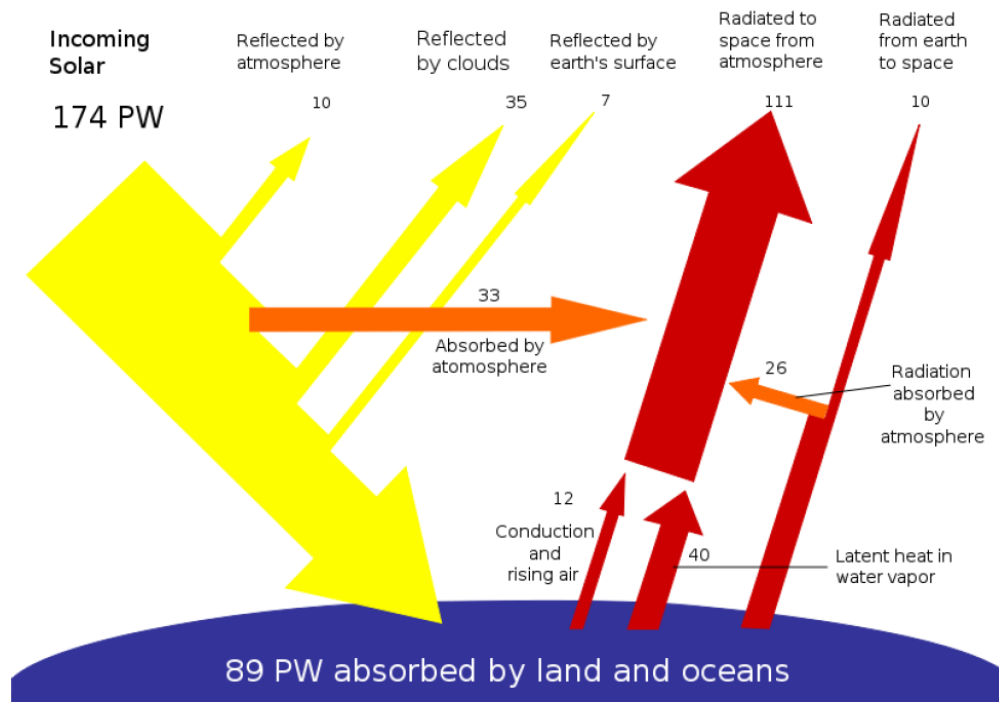


Figure 2.1 Solar radiation distribution [18].

From the above Figure 2.1 of solar radiation, Earth receives 174 petawatts (PW) of incoming solar radiation at the upper atmosphere. Approximately 30% is reflected back to space and only 89 pw is absorbed by oceans and land masses. The spectrum of solar light at the Earth's surface is generally spread across the visible and near-infrared region with a small part in the near-ultraviolet. The total solar energy absorbed by Earth's atmosphere, oceans and land masses is approximately 3,850,000 EJ per year [13].

2.4 Solar Radiation Reaching Earth Surface

The intensity of solar radiation reaching earth surface which is 1369 watts per square meter is known as Solar Constant. It is important to realize that it is not the intensity per square meter of the Earth's surface but per square meter on a sphere with the radius of 149,596,000 km and with the Sun at its center.

The total amount solar radiation intercepted by the Earth is the Solar Constant multiplied by the cross section area of the Earth. If we now divide the calculated number by the surface area of the Earth, we shall find how much solar radiation is received in an average per square meter of the Earth's surface [10]. Hence the average solar radiation R per square meter of the Earth surface is,

$$R = \frac{S \times \pi r^2}{4 \times \pi r^2} = \frac{1369}{4} = \text{approx. } 342 \frac{W}{m^2} \quad (2.1)$$

where S is the solar constant ($1369 \frac{W}{m^2}$), r is the earth radius.

The Handy formula which is used to calculate solar energy received by earth

$$E = 3.6 \times (10^{-9}) * S * n * r^2 \quad (2.2)$$

where E is the solar energy in EJ.

S is the Solar Constant in W/m^2 .

n is the number of hours.

r is the Earth's radius in km [10].

2.5 Spectrum of Sun

The performance of Photovoltaic device is reliant on the spectral distribution of solar radiation. The standard spectral distribution is mainly used as reference for evaluation of PV devices. There are two standard terrestrial distribution defined by the American Society for Testing and Materials (ASTM), global AM1.5 and direct normal. The solar radiation that is perpendicular to a plane directly facing the sun is known as direct normal. The global corresponds to the spectrum of the diffuse radiations. Diffuse radiations are the radiations which are reflected on earth's surface or influenced by atmospheric conditions. To measure the global radiations an instrument named pyranometer is used. This instrument is designed in such a way that it responds to each wavelengths and so that we get a precise value for total power in any incident spectrum [5].

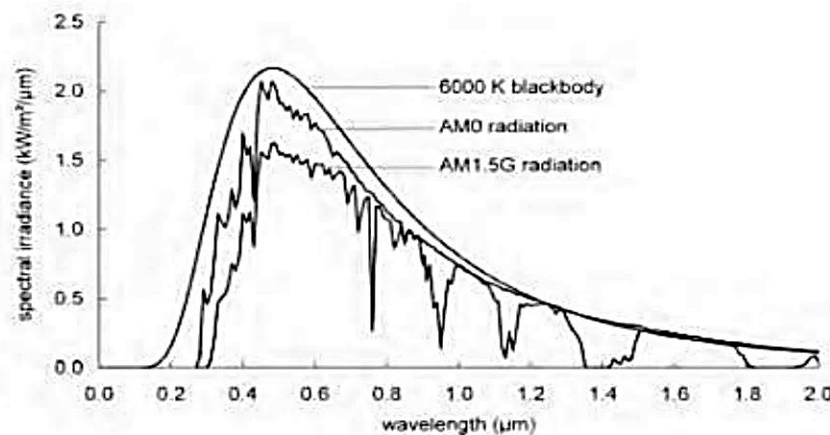


Figure 2.2 Spectral distribution of black body radiation and sun radiation [11].

The AM initials in the above Figure stands for air mass. The air mass in this circumstance means the mass of air between a surface and the sun [6]. The length of the path of solar radiation from the sun through the atmosphere is indicated by the number AM_x . The longer the path the more is the deviation of light. The AM_0 in the above figure means the spectral distribution and intensity of sunlight in near-earth space without atmospheric attenuation [6].

2.6 Standard Test Conditions (STC)

The comparison between different photovoltaic cells can be done on the basis of their performance and characteristic curve. The parameters are always given in datasheet. The datasheet makes available the notable parameter regarding the characteristics and performance of PV cells with respect to standard test condition.

Standard test conditions are as follows:

Temperature (T_n) = 25°C

Irradiance (G_n) = 1000 W/m²

Spectrum of $x = 1.5$ i.e. AM.

Chapter 3

Photovoltaic Cell

3.1 Definition

A photovoltaic system is a system which uses one or more solar panels to convert solar energy into electricity. It consists of multiple components, including the photovoltaic modules, mechanical and electrical connections and mountings and means of regulating and/or modifying the electrical output [14].

3.2 Photovoltaic Arrangements

3.2.1 Photovoltaic Cell

PV cells are made of semiconductor materials, such as silicon. For solar cells, a thin semiconductor wafer is specially treated to form an electric field, positive on one side and negative on the other. When light energy strikes the solar cell, electrons are knocked loose from the atoms in the semiconductor material. If electrical conductors are attached to the positive and negative sides, forming an electrical circuit, the electrons can be captured in the form of an electric current - that is, electricity. This electricity can then be used to power a load [16]. A PV cell can either be circular or square in construction.

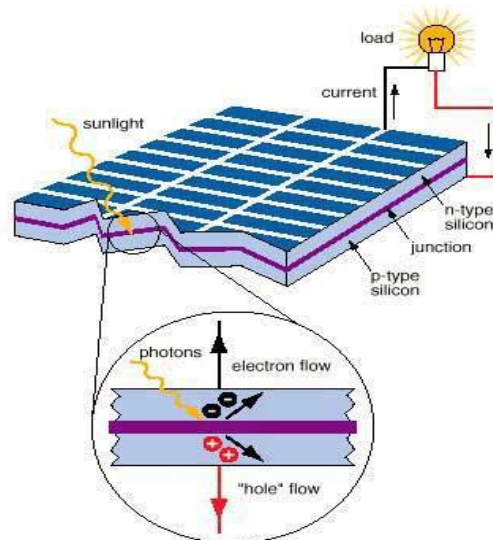


Figure 3.1 Basic Structure of PV Cell

3.2.2 Photovoltaic Module

Due to the low voltage generated in a PV cell (around 0.5V), several PV cells are connected in series (for high voltage) and in parallel (for high current) to form a PV module for desired output. Separate diodes may be needed to avoid reverse currents, in case of partial or total shading, and at night. The p-n junctions of mono-crystalline silicon cells may have adequate reverse current characteristics and these are not necessary. Reverse currents waste power and can also lead to overheating of shaded cells. Solar cells become less efficient at higher temperatures and installers try to provide good ventilation behind solar panels [15].

3.2.3 Photovoltaic Array

The power that one module can produce is not sufficient to meet the requirements of home or business. Most PV arrays use an inverter to convert the DC power into alternating current that can power the motors, loads, lights etc. The modules in a PV array are usually first connected in series to obtain the desired voltages; the individual modules are then connected in parallel to allow the system to produce more current [14].

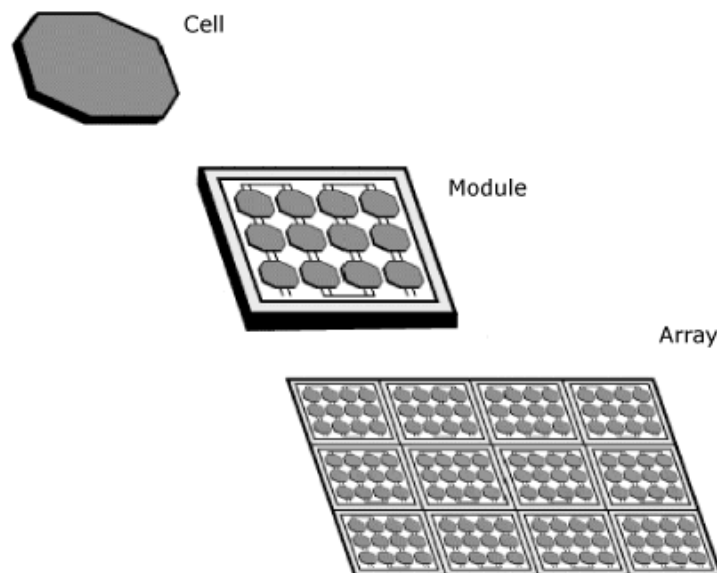


Figure 3.2 Photovoltaic system [16]

3.3 Materials Used in PV Cell

The materials used in PV cells are as follows:

Single-crystal silicon

Single-crystal silicon cells are the most common in the PV industry. The main technique for producing single-crystal silicon is the Czochralski (CZ) method. High-purity polycrystalline is melted in a quartz crucible. A single-crystal silicon seed is dipped into this molten mass of polycrystalline. As the seed is pulled slowly from the melt, a single-crystal ingot is formed. The ingots are then sawed into thin wafers about 200-400 micrometers thick (1 micrometer = 1/1,000,000 meter). The thin wafers are then polished, doped, coated, interconnected and assembled into modules and arrays [7].

Polycrystalline silicon

Consisting of small grains of single-crystal silicon, polycrystalline PV cells are less energy efficient than single-crystalline silicon PV cells. The grain boundaries in polycrystalline silicon hinder the flow of electrons and reduce the power output of the cell. A common approach to produce polycrystalline silicon PV cells is to slice thin wafers from blocks of cast polycrystalline silicon. Another more advanced approach is the “ribbon growth” method in which silicon is grown directly as thin ribbons or sheets with the approach thickness for making PV cells [7].

Gallium Arsenide (GaAs)

A compound semiconductor made of two elements: Gallium (Ga) and Arsenic (As). GaAs has a crystal structure similar to that of silicon. An advantage of GaAs is that it has high level of light absorptivity. To absorb the same amount of sunlight, GaAs requires only a layer of few micrometers thick while crystalline silicon requires a wafer of about 200-300 micrometers thick. Also, GaAs has much higher energy conversion efficiency than crystal

silicon, reaching about 25 to 30%. The only drawback of GaAs PV cells is the high cost of single crystal substrate that GaAs is grown on [7].

Cadmium Telluride (CdTe)

It is a polycrystalline compound made of cadmium and telluride with a high light absorptivity capacity (i.e a small thin layer of the compound can absorb 90% of solar irradiation). The main disadvantage of this compound is that the instability of PV cell or module performance. As it a toxic substance, the manufacturing process should be done by extra precaution [7].

Copper Indium Diselenide (CuInSe₂)

It is a polycrystalline compound semiconductor made of copper, indium and selenium. It delivers high energy conversion efficiency without suffering from outdoor degradation problem. It is one of the most light-absorbent semiconductors. As it is a complex material and toxic in nature so the manufacturing process face some problem [7].

3.4 Characteristics of PV Cell

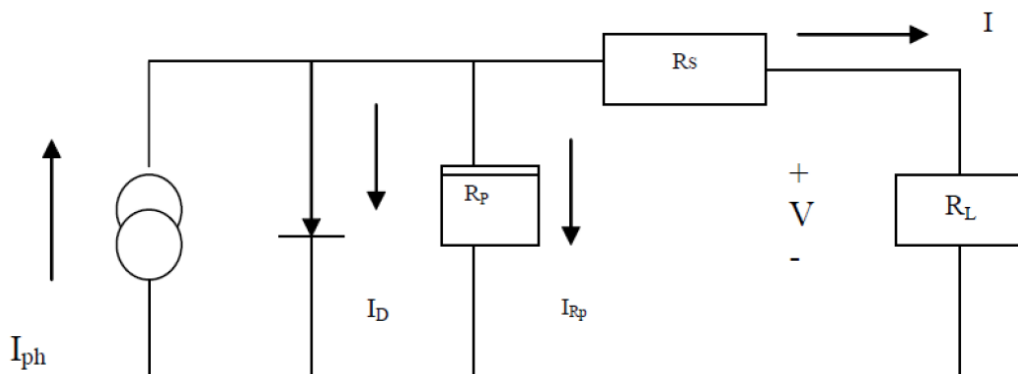


Figure 3.3 Equivalent circuit of a PV cell

An ideal is modeled by a current source in parallel with a diode. However, no solar cell is ideal and thereby shunt and series resistances are added to the model as shown in the PV cell diagram above. R_S is the intrinsic series resistance whose value is very small. R_P is the equivalent shunt resistance which has a very high value [4].

Applying Kirchoff's law to the node where I_{ph} , diode, R_p and R_s meet, we get

$$I_{ph} = I_D + I_{Rp} + I \quad (3.1)$$

We get the following equation for the photovoltaic current:

$$I = I_{ph} - I_{Rp} - I_D \quad (3.2)$$

$$I = I_{ph} - I_0 \cdot \left[\exp\left(\frac{V + I \cdot R_s}{V_T}\right) - 1 \right] - \left[\frac{V + I \cdot R_s}{R_p} \right] \quad (3.3)$$

Where, I_{ph} is the Insolation current, I is the Cell current, I_0 is the Reverse saturation current, V is the Cell voltage, R_s is the Series resistance, R_p is the Parallel resistance, V_T is the Thermal voltage (KT/q), K is the Boltzman constant, T is the Temperature in Kelvin, q is the Charge of an electron.

3.4.1 Efficiency of PV Cell

The efficiency of a PV cell is defined as the ratio of peak power to input solar power.

$$\eta = \frac{V_{mp} \cdot I_{mp}}{I \left(\frac{KW}{m^2} \right) \cdot A(m^2)} \quad (3.4)$$

where, V_{mp} is the voltage at peak power, I_{mp} is the current at peak power, I is the solar intensity per square metre, A is the area on which solar radiation fall.

The efficiency will be maximum if we track the maximum power from the PV system at different environmental condition such as solar irradiance and temperature by using different methods for maximum power point tracking.

3.5 Modelling of PV Array:

The building block of PV arrays is the solar cell, which is basically a p-n junction that directly converts light energy into electricity: it has an equivalent circuit as shown below in Figure 3.4.

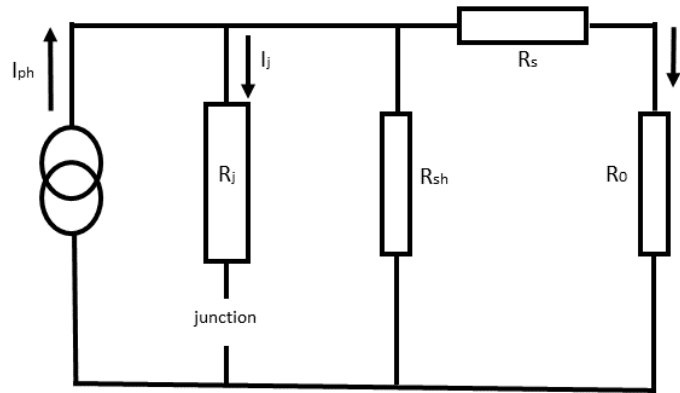


Figure 3.4 Equivalent circuit of a PV cell

The current source I_{ph} represents the cell photo current; R_j is used to represent the non-linear impedance of the p-n junction; R_{sh} and R_s are used to represent the intrinsic series and shunt resistance of the cell respectively. Usually the value of R_{sh} is very large and that of R_s is very small, hence they may be neglected to simplify the analysis. PV cells are grouped in larger units called PV modules which are further interconnected in series-parallel configuration to form PV arrays or PV generators [3]. The PV mathematical model used to simplify our PV array is represented by the equation:

$$I = n_p I_{ph} - n_p I_{rs} \left[\exp\left(\frac{q}{KTA} * \frac{V}{n_s}\right) - 1 \right] \quad (3.5)$$

where I is the PV array output current; V is the PV array output voltage; n_s is the number of cells in series and n_p is the number of cells in parallel; q is the charge of an electron; k is the Boltzmann's constant; A is the p-n junction ideality factor; T is the cell temperature (K); I_{rs} is the cell reverse saturation current. The factor A in equation (3.5) determines the

cell deviation from the ideal p-n junction characteristics; it ranges between 1-5 but for our case $A=2.46$ [3].

The cell reverse saturation current I_{rs} varies with temperature according to the following equation:

$$I_{rs}=I_{rr}\left[\frac{T}{T_r}\right]^3 \exp\left(\frac{qE_G}{KA} \left[\frac{1}{T_r}-\frac{1}{T}\right]\right) \quad (3.6)$$

Where T_r is the cell reference temperature, I_{rr} is the cell reverse saturation temperature at T_r and E_G is the band gap of the semiconductor used in the cell.

The temperature dependence of the energy gap of the semi conductor is given by [20]:

$$E_G= E_G(0)-\frac{\alpha T^2}{T+\beta} \quad (3.7)$$

The photo current I_{ph} depends on the solar radiation and cell temperature as follows:

$$I_{ph}=[I_{scr} + K_i(T - T_r)] \frac{S}{100} \quad (3.8)$$

where I_{scr} is the cell short-circuit current at reference temperature and radiation, K_i is the short circuit current temperature coefficient, and S is the solar radiation in mW/cm^2 . The PV power can be calculated using equation (3.5) as follows:

$$P=IV= n_p I_{ph} V \left[\left(\frac{q}{KTA} * \frac{V}{n_s} \right) - 1 \right] \quad (3.9)$$

3.5.1 PV Array Characteristic Curves

The current to voltage characteristic of a solar array is non-linear, which makes it difficult to determine the MPP. The Figure below gives the characteristic I-V and P-V curve for fixed level of solar irradiation and temperature.

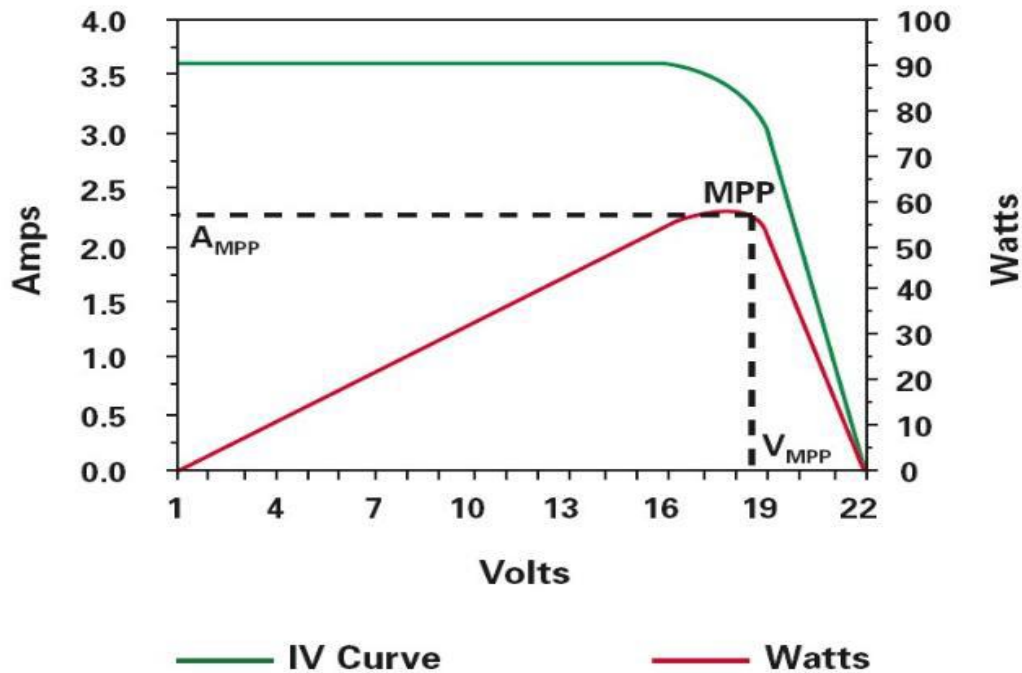


Figure 3.5 I-V and PV curve characteristics [19].

The IV and PV curves for various irradiance but a fixed temperature (250C) is shown below in Figure (3.6) & (3.7). The characteristic I-V curve tells that there are two regions in the curve: one is the current source region and another is the voltage source region. In the voltage source region (in the right side of the curve), the internal impedance is low and in the current source region (in the left side of the curve), the impedance is high. Irradiance temperature plays an important role in predicting the I-V characteristic, and effects of both factors have to be considered while designing the PV system. Whereas the irradiance affects the output, temperature mainly affects the terminal voltage. The figures (3.8), (3.9) gives the simulated I-V and P-V characteristic for various temperatures at a fixed irradiance at 1000 W/m² [4].

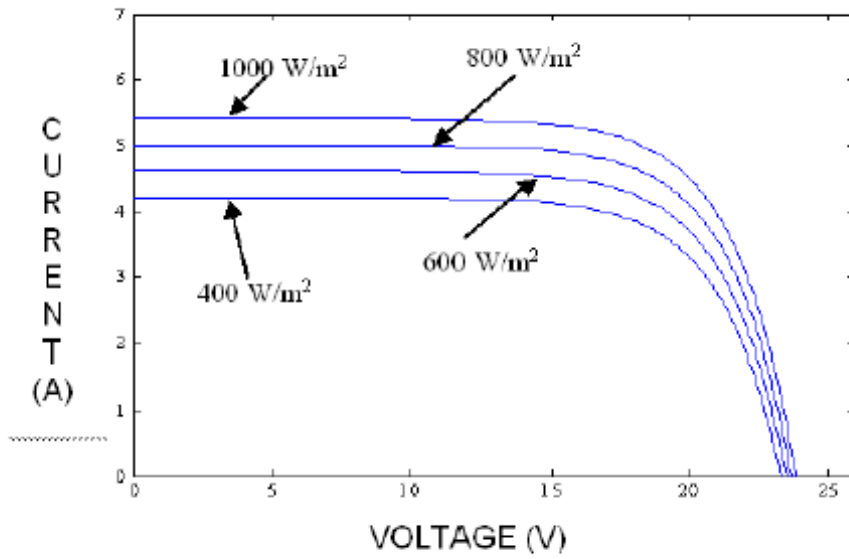


Figure 3.6 I-V characteristic of a solar array for a fixed temperature but varying irradiance

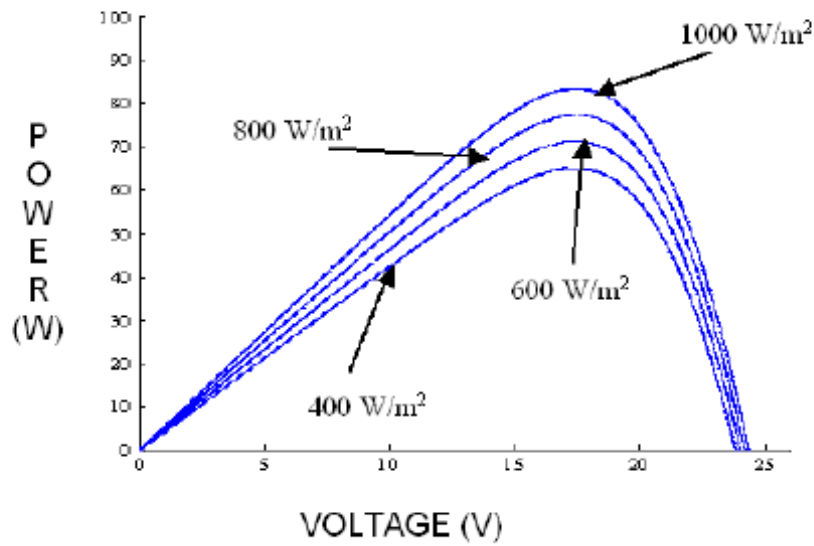


Figure 3.7 P-V characteristic of a solar array for a fixed temperature but varying irradiance

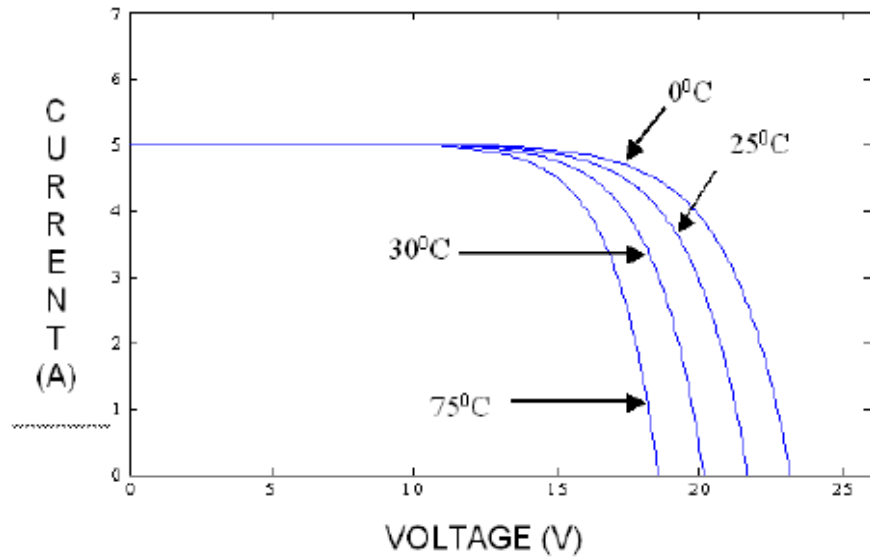


Figure 3.8 I-V Characteristic of a PV array under a fixed irradiance but varying temperatures

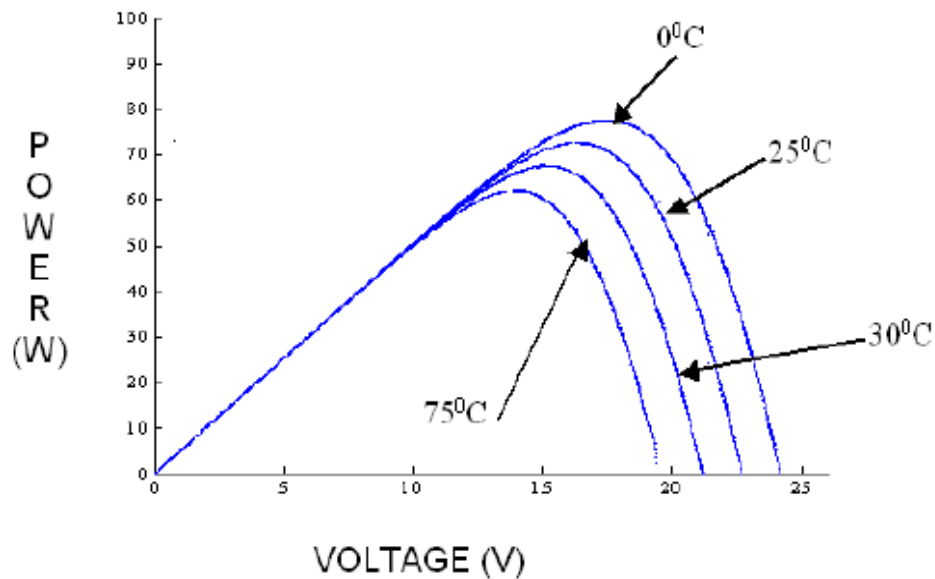


Figure 3.9 P-V Characteristic of a PV array under a fixed irradiance but varying temperatures.

From the I-V, we observe that the short circuit current increases with increase in irradiance at a fixed temperature. Moreover, from the I-V and P-V curves at a fixed irradiance, it is observed that the open circuit voltage decreases with increase in temperature.

Chapter 4

Converters

DC-DC Converters

DC-DC converters can be used as switching mode regulators to convert an unregulated dc voltage to a regulated dc output voltage. The regulation is normally achieved by PWM at a fixed frequency and the switching device is generally BJT, MOSFET or IGBT. The minimum oscillator frequency should be about 100 times longer than the transistor switching time to maximize efficiency. This limitation is due to the switching loss in the transistor. The transistor switching loss increases with the switching frequency and thereby, the efficiency decreases. There are four topologies for the switching regulators: buck converter, boost converter, buck-boost converter, cuk converter. However, this project work deals with the buck and boost regulator and further discussions will be concentrated towards these converters.

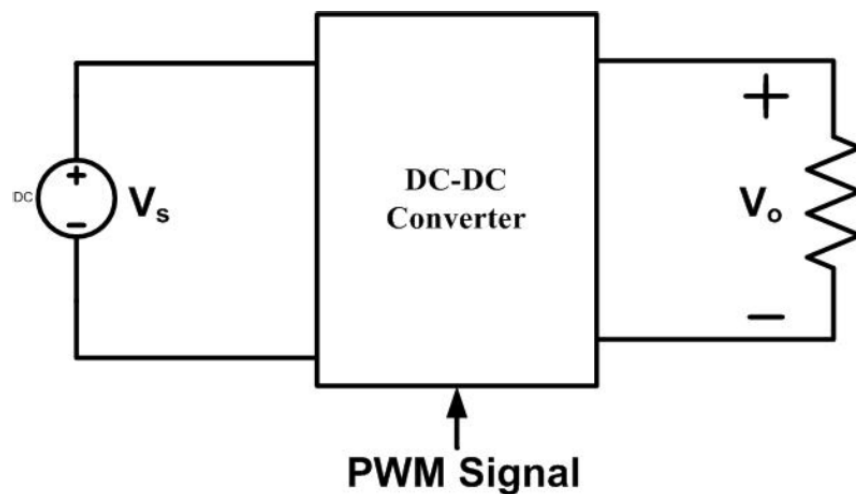


Figure 4.1 Block Diagram of DC-DC Converter.

4.1 Buck Converter

A buck converter (step-down converter) is a DC-to-DC power converter which steps down voltage (while stepping up current) from its input (supply) to its output (load). It is a class of switched-mode power supply (SMPS) typically containing at least two semiconductors (a diode and a transistor, although modern buck converters frequently replace the diode with a second transistor used for synchronous rectification) and at least one energy storage element, a capacitor, inductor, or the two in combination. To reduce voltage ripple, filters made of capacitors (sometimes in combination with inductors) are normally added to such a converter's output (load-side filter) and input (supply-side filter).

Switching converters (such as buck converters) provide much greater power efficiency as DC-to-DC converters than linear regulators, which are simpler circuits that lower voltages by dissipating power as heat, but do not step up output current.

Buck converters can be highly efficient (often higher than 90%), making them useful for tasks such as converting a computer's main (bulk) supply voltage (often 12 V) down to lower voltages needed by USB, DRAM and the CPU (1.8 V or less).

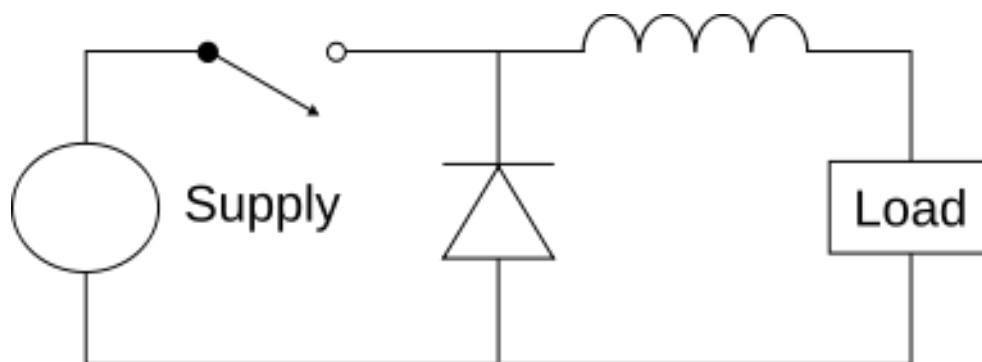


Figure 4.2 Buck Converter Circuit Diagram.

4.1.1 Theory of Operation of Buck Converter

The basic operation of the buck converter has the current in an inductor controlled by two switches (usually a transistor and a diode). In the idealized converter, all the components are considered to be perfect. Specifically, the switch and the diode have zero voltage drop when on and zero current flow when off, and the inductor has zero series resistance. Further, it is assumed that the input and output voltages do not change over the course of a cycle (this would imply the output capacitance as being infinite).

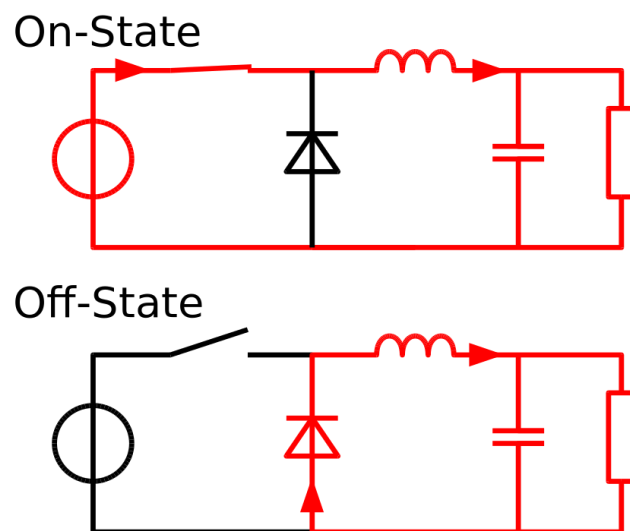


Figure 4.3 The two circuit configurations of a buck converter: on-state, when the switch is closed; and off-state, when the switch is open (arrows indicate current according to the direction conventional current model).

The conceptual model of the buck converter is best understood in terms of the relation between current and voltage of the inductor. Beginning with the switch open (off-state), the current in the circuit is zero. When the switch is first closed (on-state), the current will begin to increase, and the inductor will produce an opposing voltage across its terminals in response to the changing current. This voltage drop counteracts the voltage of the source and therefore reduces the net voltage across the load. Over time, the rate of change of

current decreases, and the voltage across the inductor also then decreases, increasing the voltage at the load. During this time, the inductor stores energy in the form of a magnetic field. If the switch is opened while the current is still changing, then there will always be a voltage drop across the inductor, so the net voltage at the load will always be less than the input voltage source. When the switch is opened again (off-state), the voltage source will be removed from the circuit, and the current will decrease. The decreasing current will produce a voltage drop across the inductor (opposite to the drop at on-state), and now the inductor becomes a Current Source. The stored energy in the inductor's magnetic field supports the current flow through the load. This current, flowing while the input voltage source is disconnected, when concatenated with the current flowing during on-state, totals to current greater than the average input current (being zero during off-state). The "increase" in average current makes up for the reduction in voltage, and ideally preserves the power provided to the load. During the off-state, the inductor is discharging its stored energy into the rest of the circuit. If the switch is closed again before the inductor fully discharges (on-state), the voltage at the load will always be greater than zero.

Continuous mode

Buck converter operates in continuous mode if the current through the inductor (I_L) never falls to zero during the commutation cycle. In this mode, the operating principle is described by the plots in figure 4.4:

- When the switch pictured above is closed (top of figure 4.3), the voltage across the inductor is $V_L = V_i - V_o$. The current through the inductor rises linearly (in approximation, so long as the voltage drop is almost constant). As the diode is reverse-biased by the voltage source V , no current flows through it;
- When the switch is opened (bottom of figure 4.3), the diode is forward biased. The voltage across the inductor is $V_L = -V_o$. Current I_L decreases.

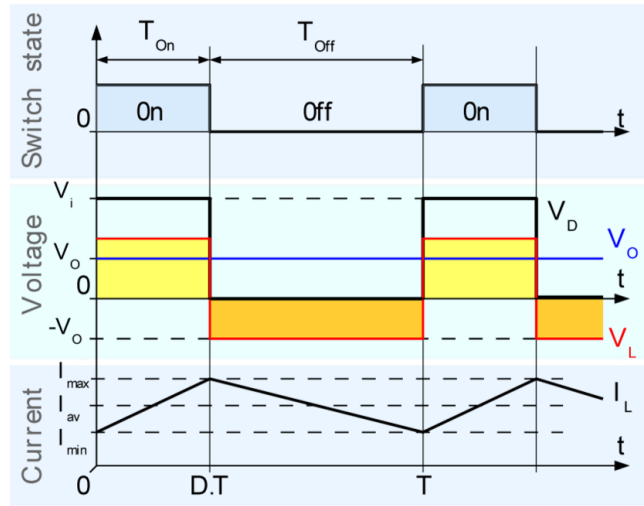


Figure 4.4: Evolution of the voltages and currents with time in an ideal buck converter operating in continuous mode.

The energy stored in inductor L is

$$E = \frac{1}{2}LI_L^2 \quad (4.1)$$

Therefore, it can be seen that the energy stored in L increases during on-time as I_L increases and then decreases during the off-state. L is used to transfer energy from the input to the output of the converter.

The rate of change of I_L can be calculated from:

$$V_L = L \frac{dI_L}{dt} \quad (4.2)$$

With V_L equal to $V_i - V_o$ during the on-state and to $-V_o$ during the off-state. Therefore, the increase in current during the on-state is given by:

$$\Delta I_{L_{or}} = \int_0^{t_{on}} \frac{V_L}{L} dt = \frac{(V_i - V_o)}{L} t_{on}, \quad t_{on} = DT \quad (4.3)$$

where D is a scalar called the duty cycle with a value between 0 and 1.

Conversely, the decrease in current during the off-state is given by:

$$\Delta I_{L_{\text{off}}} = \int_{t_{\text{on}}}^{T=t_{\text{on}}+t_{\text{off}}} \frac{V_L}{L} dt = -\frac{V_o}{L} t_{\text{off}}, \quad t_{\text{off}} = (1 - D)T \quad (4.4)$$

If we assume that the converter operates in the steady state, the energy stored in each component at the end of a commutation cycle T is equal to that at the beginning of the cycle.

That means that the current I_L is the same at $T=0$ and at $T=T$ (figure 4.4).

So we can write from the above equations:

$$\begin{aligned} \Delta I_{L_{\text{on}}} + \Delta I_{L_{\text{off}}} &= 0 \\ \frac{V_i - V_o}{L} t_{\text{on}} - \frac{V_o}{L} t_{\text{off}} &= 0 \end{aligned} \quad (4.5)$$

The above integrations can be done graphically. In figure 4.4, $\Delta I_{L_{\text{on}}}$ is proportional to the area of the yellow surface, and $\Delta I_{L_{\text{off}}}$ to the area of the orange surface, as these surfaces are defined by the inductor voltage (red lines). As these surfaces are simple rectangles, their areas can be found easily: $(V_i - V_o) t_{\text{on}}$ for the yellow rectangle and $-V_o t_{\text{off}}$ for the orange one. For steady state operation, these areas must be equal.

As can be seen in figure 4.4, $t_{\text{on}} = DT$ and $t_{\text{off}} = (1-D)T$.

This yields:

$$D = \frac{V_o}{V_i} \quad (4.6)$$

From this equation, it can be seen that the output voltage of the converter varies linearly with the duty cycle for a given input voltage. As the duty cycle D is equal to the ratio between t_{on} and the period T , it cannot be more than 1. Therefore, $V_o \leq V_i$.

This is why this converter is referred to as step-down converter.

So, for example, stepping 12 V down to 3 V (output voltage equal to one quarter of the input voltage) would require a duty cycle of 25%, in our theoretically ideal circuit.

4.2 Boost Converter

A boost converter (step-up converter) is a DC-to-DC power converter that steps up voltage (while stepping down current) from its input (supply) to its output (load). It is a class of switched-mode power supply (SMPS) containing at least two semiconductors (a diode and a transistor) and at least one energy storage element: a capacitor, inductor, or the two in combination. To reduce voltage ripple, filters made of capacitors (sometimes in combination with inductors) are normally added to such a converter's output (load-side filter) and input (supply-side filter).

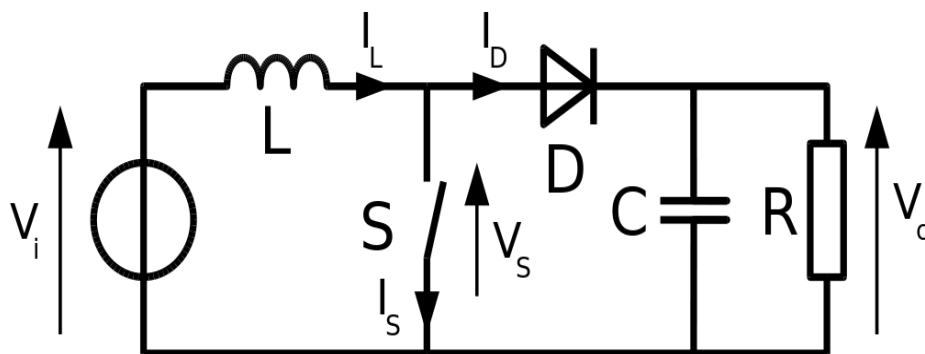


Figure 4.5 Boost Converter Circuit Diagram.

4.2.1 Theory of Operation of Boost Converter

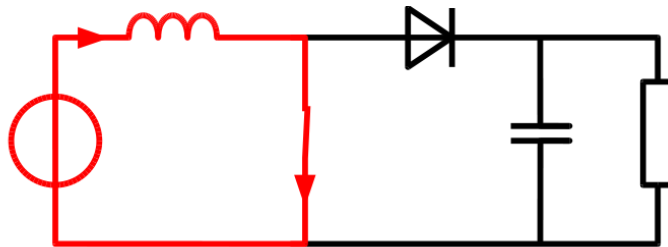
The key principle that drives the boost converter is the tendency of an inductor to resist changes in current by creating and destroying a magnetic field. In a boost converter, the output voltage is always higher than the input voltage. A schematic of a boost power stage is shown in Figure 1.

(a) When the switch is closed, current flows through the inductor in clockwise direction and the inductor stores some energy by generating a magnetic field. Polarity of the left side of the inductor is positive.

(b) When the switch is opened, current will be reduced as the impedance is higher. The magnetic field previously created will be destroyed to maintain the current towards the load. Thus the polarity will be reversed (means left side of inductor will be negative now). As a result, two sources will be in series causing a higher voltage to charge the capacitor through the diode D.

While the switch is opened, the capacitor in parallel with the load is charged to this combined voltage. When the switch is then closed and the right hand side is shorted out from the left hand side, the capacitor is therefore able to provide the voltage and energy to the load. During this time, the blocking diode prevents the capacitor from discharging through the switch.

ON State



OFF State

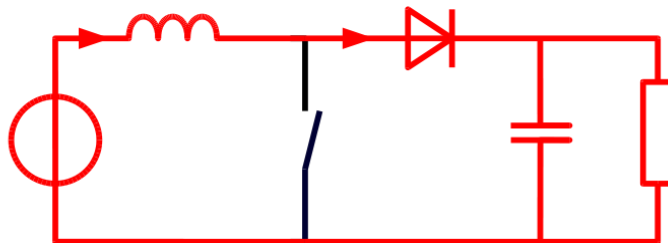


Figure 4.6 The two circuit configurations of a boost converter: on-state, when the switch is closed; and off-state, when the switch is open (arrows indicate current according to the direction conventional current model).

The basic principle of a Boost converter consists of 2 distinct states (see figure 4.8):

- i. In the On-state, the switch S is closed, resulting in an increase in the inductor current;
- ii. In the Off-state, the switch is open and the only path offered to inductor current is through the flyback diode D, the capacitor C and the load R. This results in transferring the energy accumulated during the On-state into the capacitor.

Continuous Mode

When a boost converter operates in continuous mode, the current through the inductor (I_L) never falls to zero. Figure 3 shows the typical waveforms of currents and voltages in a converter operating in this mode. The output voltage can be calculated as follows, in the case of an ideal converter (i.e. using components with an ideal behavior) operating in steady conditions.

During the On-state, the switch S is closed, which makes the input voltage (V_i) appear across the inductor, which causes a change in current (I_L) flowing through the inductor during a time period (t) by the formula:

$$\frac{\Delta I_L}{\Delta t} = \frac{V_i}{L} \quad (4.7)$$

Where L is the inductor value.

At the end of the On-state, the increase of I_L is therefore:

$$\Delta I_{L_{On}} = \frac{1}{L} \int_0^{DT} V_i dt = \frac{DT}{L} V_i \quad (4.8)$$

D is the duty cycle. It represents the fraction of the commutation period T during which the switch is On. Therefore, D ranges between 0 (S is never on) and 1 (S is always on).

During the Off-state, the switch S is open, so the inductor current flows through the load. If we consider zero voltage drop in the diode, and a capacitor large enough for its voltage to remain constant, the evolution of I_L is:

$$V_i - V_o = L \frac{dI_L}{dt} \quad (4.9)$$

Therefore, the variation of I_L during the Off-period is:

$$\Delta I_{L_{Off}} = \int_{DT}^T \frac{(V_i - V_o) dt}{L} = \frac{(V_i - V_o)(1 - D)T}{L} \quad (4.10)$$

As we consider that the converter operates in steady-state conditions, the amount of energy stored in each of its components has to be the same at the beginning and at the end of a commutation cycle. In particular, the energy stored in the inductor is given by:

$$E = \frac{1}{2} L I_L^2 \quad (4.11)$$

So, the inductor current has to be the same at the start and end of the commutation cycle. This means the overall change in the current (the sum of the changes) is zero:

$$\Delta I_{L_{On}} + \Delta I_{L_{Off}} = 0 \quad (4.12)$$

Substituting $\Delta I_{L_{On}}$ and $\Delta I_{L_{Off}}$ by their expressions yields:

$$\Delta I_{L_{On}} + \Delta I_{L_{Off}} = \frac{V_i DT}{L} + \frac{(V_i - V_o)(1 - D)T}{L} = 0 \quad (4.13)$$

This can be written as:

$$\frac{V_o}{V_i} = \frac{1}{1 - D} \quad (4.14)$$

The above equation shows that the output voltage is always higher than the input voltage (as the duty cycle goes from 0 to 1), and that it increases with D, theoretically to infinity

as D approaches 1. This is why this converter is sometimes referred to as a step-up converter.

Rearranging the equation reveals the duty cycle to be:

$$D = 1 - \frac{V_i}{V_o} \tag{4.15}$$

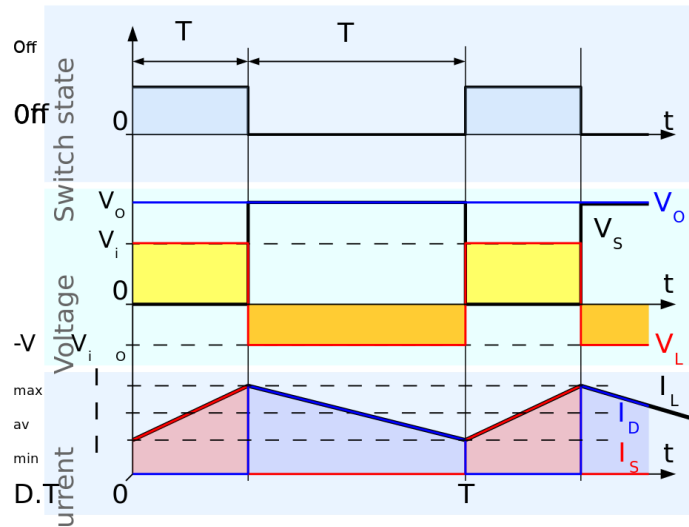


Figure 4.7 Waveforms of current and voltage in a boost converter operating in continuous mode.

Chapter 5

PID Integration

A proportional–integral–derivative controller (PID controller or three term controller) is a control loop feedback mechanism widely used in industrial control systems and a variety of other applications requiring continuously modulated control. A PID controller continuously calculates an error value $e(t)$ as the difference between a desired setpoint (SP) and a measured process variable (PV) and applies a correction based on proportional, integral, and derivative terms (denoted P , I , and D respectively), hence the name.

In practical terms it automatically applies accurate and responsive correction to a control function. An everyday example is the cruise control on a car; where external influences such as hills (gradients) would decrease speed. The PID algorithm restores from current speed to the desired speed in an optimal way, without delay or overshoot, by controlling the power output of the vehicle's engine.

The first theoretical analysis and practical application was in the field of automatic steering systems for ships, developed from the early 1920s onwards. It was then used for automatic process control in manufacturing industry, where it was widely implemented in pneumatic, and then electronic, controllers. Today there is universal use of the PID concept in applications requiring accurate and optimized automatic control.

5.1 Fundamental operation of PID controller

The distinguishing feature of the PID controller is the ability to use the three control terms of proportional, integral and derivative influence on the controller output to apply accurate and optimal control. The block diagram on the right shows the principles of how these terms are generated and applied. It shows a PID controller, which continuously calculates an error value $e(t)$ as the difference between a desired setpoint $SP = r(t)$ and a

measured process variable $PV = y(t)$, and applies a correction based on proportional, integral, and derivative terms. The controller attempts to minimize the error over time by adjustment of a control variable $u(t)$, such as the opening of a control valve, to a new value determined by a weighted sum of the control terms.

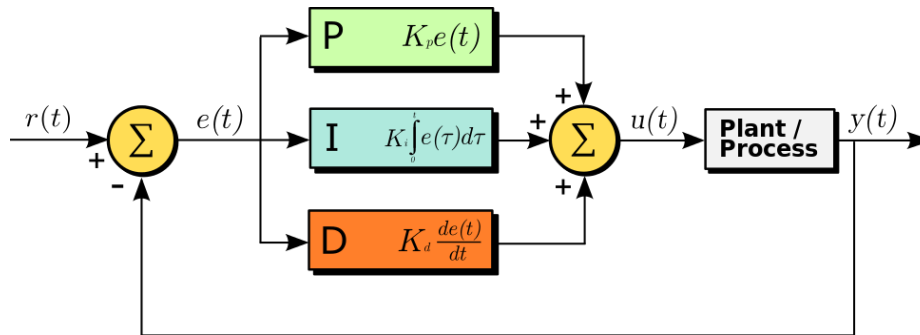


Figure 5.1 A block diagram of a PID controller in a feedback loop. $r(t)$ is the desired process value or setpoint (SP), and $y(t)$ is the measured process value (PV).

In this model:

- i. Term **P** is proportional to the current value of the SP – PV error $e(t)$. For example, if the error is large and positive, the control output will be proportionately large and positive, taking into account the gain factor "K". Using proportional control alone in a process with compensation such as temperature control, will result in an error between the setpoint and the actual process value, because it requires an error to generate the proportional response. If there is no error, there is no corrective response.
- ii. Term **I** accounts for past values of the SP – PV error and integrates them over time to produce the I term. For example, if there is a residual SP – PV error after the application of proportional control, the integral term seeks to eliminate the residual error by adding a control effect due to the historic cumulative value of the error. When the error is eliminated, the integral term will cease to grow. This will result

in the proportional effect diminishing as the error decreases, but this is compensated for by the growing integral effect.

- iii. Term **D** is a best estimate of the future trend of the SP – PV error, based on its current rate of change. It is sometimes called "anticipatory control", as it is effectively seeking to reduce the effect of the SP – PV error by exerting a control influence generated by the rate of error change. The more rapid the change, the greater the controlling or dampening effect.

Tuning – The balance of these effects is achieved by "loop tuning" (see later) to produce the optimal control function. The tuning constants are shown below as "K" and must be derived for each control application, as they depend on the response characteristics of the complete loop external to the controller. These are dependent on the behavior of the measuring sensor, the final control element (such as a control valve), any control signal delays and the process itself. Approximate values of constants can usually be initially entered knowing the type of application, but they are normally refined, or tuned, by "bumping" the process in practice by introducing a setpoint change and observing the system response.

Control action – The mathematical model and practical loop above both use a "direct" control action for all the terms, which means an increasing positive error results in an increasing positive control output for the summed terms to apply correction. However, the output is called "reverse" acting if it is necessary to apply negative corrective action. For instance, if the valve in the flow loop was 100–0% valve opening for 0–100% control output – meaning that the controller action has to be reversed. Some process control schemes and final control elements require this reverse action. An example would be a valve for cooling water, where the fail-safe mode, in the case of loss of signal, would be

100% opening of the valve; therefore 0% controller output needs to cause 100% valve opening.

5.2 Ziegler Nichols Method

The Ziegler–Nichols tuning method is a heuristic method of tuning a PID controller. It was developed by John G. Ziegler and Nathaniel B. Nichols. It is performed by setting the *I* (integral) and *D* (derivative) gains to zero. The "P" (proportional) gain, K_p is then increased (from zero) until it reaches the ultimate gain, K_u at which the output of the control loop has stable and consistent oscillations. K_u and the oscillation period T_u are used to set the P, I, and D gains depending on the type of controller used:

Table: 5.1. Calculation of Ziegler Nichols Method

Ziegler Nichols Method			
<i>Control Type</i>	K_p	T_i	T_d
P	$0.5 K_u$	-	-
PI	$0.45 K_u$	$T_u/1.2$	-
PD	$0.8 K_u$	-	$T_u /8$
Classic PID	$0.6 K_u$	$T_u /2$	$T_u /8$
Pessen Integral Rule	$0.7 K_u$	$T_u /2.5$	$3 T_u /20$
Some Overshoot	$0.33 K_u$	$T_u /2$	$T_u /3$
No overshoot	$0.2 K_u$	$T_u /2$	$T_u /3$

The ultimate gain (K) is defined as 1/M, where M = the amplitude ratio

These 3 parameters are used to establish the correction u(t) from the error e(t) via the equation:

$$u(t) = K_p \left(e(t) + \frac{1}{T_i} \int_0^t e(\tau) d\tau + T_d \frac{de(t)}{dt} \right) \quad (5.1)$$

which has the following transfer function relationship between error and controller output:

$$u(s) = K_p \left(1 + \frac{1}{T_i s} + T_d s \right) e(s) = K_p \left(\frac{T_d T_i s^2 + T_i s + 1}{T_i s} \right) e(s) \quad (5.2)$$

Effect of proportional, integral and derivative control on close loop system is summarized in the Table 5.2. provided below.

Table: 5.2. Effect of PID on Closed Loop System

	Rise Time	Overshoot	Settling Time	Steady State Error
Proportional	Decrease	Increase	Small Change	Decrease
Integral	Decrease	Increase	Increase	Eliminate
Derivative	Small Change	Decrease	Decrease	Small Change

5.3 Control System with PID Integration

The converters displayed in Chapter 4 was of open loop system.

In control systems engineering, a system is actually a group of objects or elements capable of performing individual tasks. They are connected in a specific sequence performing a specific function. A system is of 2 types:

1. Open loop system which is also called as manual control system.
2. Closed loop system which is also named as automatic control system.

Open Loop System:

Advantages

- i. They are simpler in their layout and hence are economical and stable too due to their simplicity.
- ii. Since these are having a simple layout so are easier to construct.

Disadvantages

- i. Since these systems do not have a feedback mechanism, so they are very inaccurate in terms of result output and hence they are unreliable too.
- ii. Due to the absence of a feedback mechanism, they are unable to remove the disturbances occurring from external sources.

Closed Loop System:

Advantages:

- i. They are more accurate than open loop system due to their complex construction. They are equally accurate and are not disturbed in the presence of non-linearities.
- ii. Since they are composed of a feedback mechanism, so they clear out the errors between input and output signals, and hence remain unaffected to the external noise sources.

Disadvantages:

- i. They are relatively more complex in construction and hence it adds up to the cost making it costlier than open loop system.
- ii. Since it consists of feedback loop, it may create oscillatory response of the system and it also reduces the overall gain of the system.
- iii. It is less stable than open loop system but this disadvantage can be strikes off since we can make the sensitivity of the system very small so as to make the system as stable as possible.

5.3.1 Converters with PID Controller Integration

Earlier in Chapter 4, there were discussions about buck, boost and buck boost converter. Those were performed in open loop system. But for further improvement, closed loop system was introduced integrating PID controller as a feedback system.

It was performed for buck and boost converter. In figure 5.2, the buck converter performs in closed loop along with the PID controller there the errors are calculated and added as the feedback to reduce it in every loop.

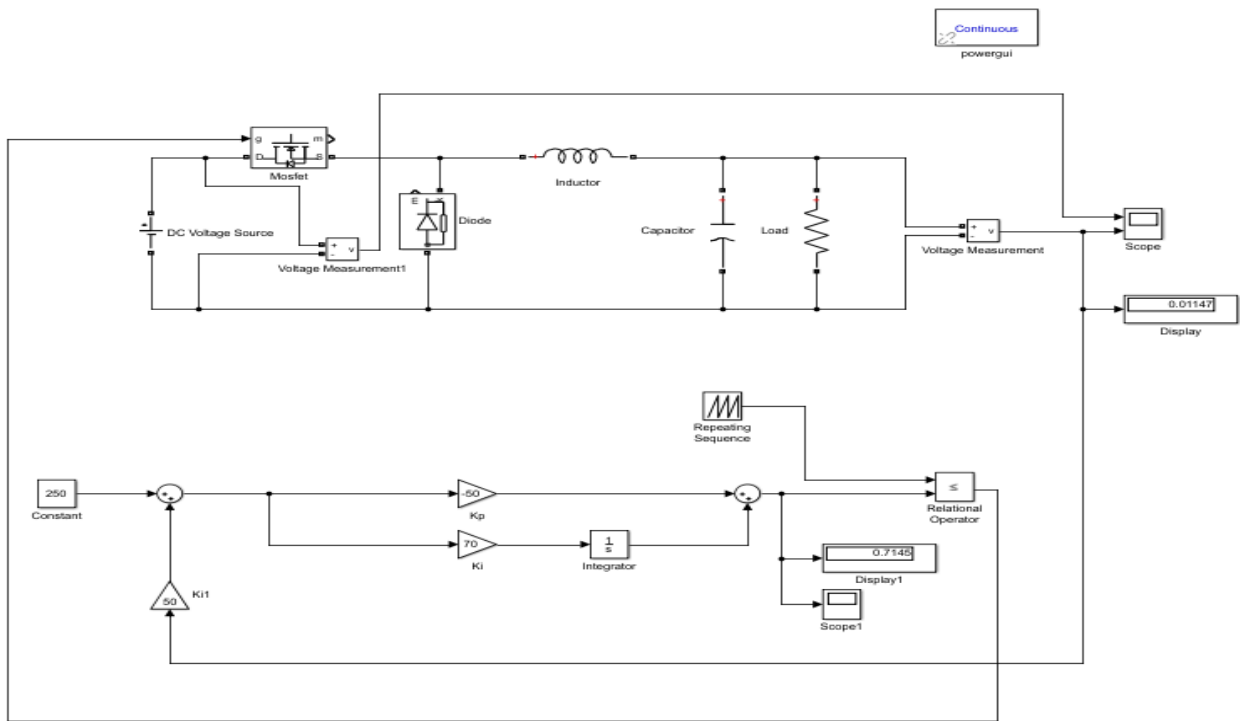


Figure 5.2: Simulink Diagram of Closed Loop Buck Converter with PID Controller.

In figure 5.3, the boost converter provides step up output in closed loop along with the PID controller there the errors are calculated and added as the feedback to reduce it in every loop.

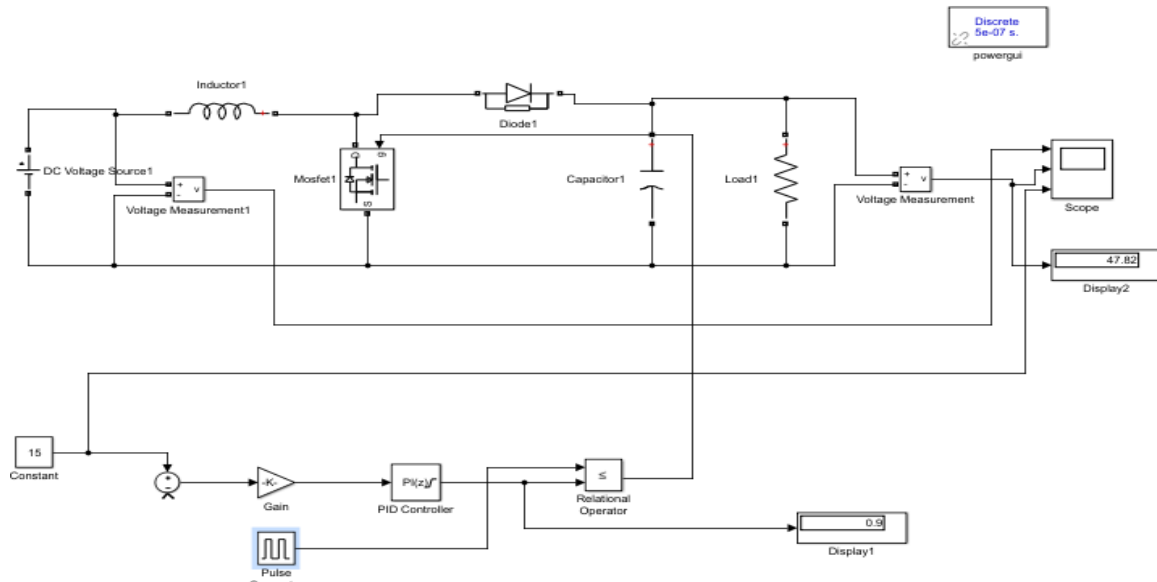


Figure 5.3: Simulink Diagram of Closed Loop Boost Converter with PID Controller.

Incorporating a PID controller with the converter improves the dynamic response and reduces the steady-state error. The derivative controller (K_D) ameliorates the transient response and the integral controller (K_I) will reduce the steady state error of the system.

5.4 Percentage Overshoot

Maximum overshoot is defined in Katsuhiko Ogata's Discrete-time control systems as "the maximum peak value of the response curve measured from the desired response of the system."

In control system theory, overshoot refers to an output exceeding its final, steady-state value. For a step input, the percentage overshoot (PO) is the maximum value minus the step value divided by the step value. In the case of the unit step, the overshoot is just the maximum value of the step response minus one. Also see the definition of overshoot in an electronics context.

For second order systems, the percentage overshoot is a function of the damping ratio ζ and is given by

$$PO = 100 \cdot e^{\left(\frac{-\zeta\pi}{\sqrt{1-\zeta^2}}\right)} \quad (5.3)$$

The damping ratio can also be found by

$$\zeta = \sqrt{\frac{\left(\ln \frac{PO}{100}\right)^2}{\pi^2 + \left(\ln \frac{PO}{100}\right)^2}} \quad (5.4)$$

In electronics, overshoot refers to the transitory values of any parameter that exceeds its final (steady state) value during its transition from one value to another. An important application of the term is to the output signal of an amplifier.

Overshoot occurs when the transitory values exceed final value. When they are lower than the final value, the phenomenon is called "undershoot".

A circuit is designed to minimize risetime while containing distortion of the signal within acceptable limits.

1. Overshoot represents a distortion of the signal.
2. In circuit design, the goals of minimizing overshoot and of decreasing circuit risetime can conflict.
3. The magnitude of overshoot depends on time through a phenomenon called "damping".
4. Overshoot often is associated with settling time; how long it takes for the output to reach steady state.

Chapter 6

Result and Simulation

Simulation was done in MATLAB-Simulink environment.

6.1.1 Parameters used in MATLAB for PV Array

The values of the parameters used in developing the MATLAB code for the Photovoltaic array have been tabled below

Table 6.1: PV Array Parameters

PARAMETERS	VALUES
N_p	4
N_s	60
I_{scr}	3.75 A
T_{r1}	40 °C
K_i	0.00023 A/K
I_{rr}	0.000021 A
K	$1.38065 * 10^{-23} J/^{\circ}K$
q	$1.6022 * 10^{-19} C$
A	2.15
E_g0	1.66 eV
α	$4.73 * 10^{-4} eV/K$
β	636 K

6.1.2 PV Array Output

The waveforms obtained by varying the solar insolation and temperatures which are fed into the PV array model have been plotted as shown below:

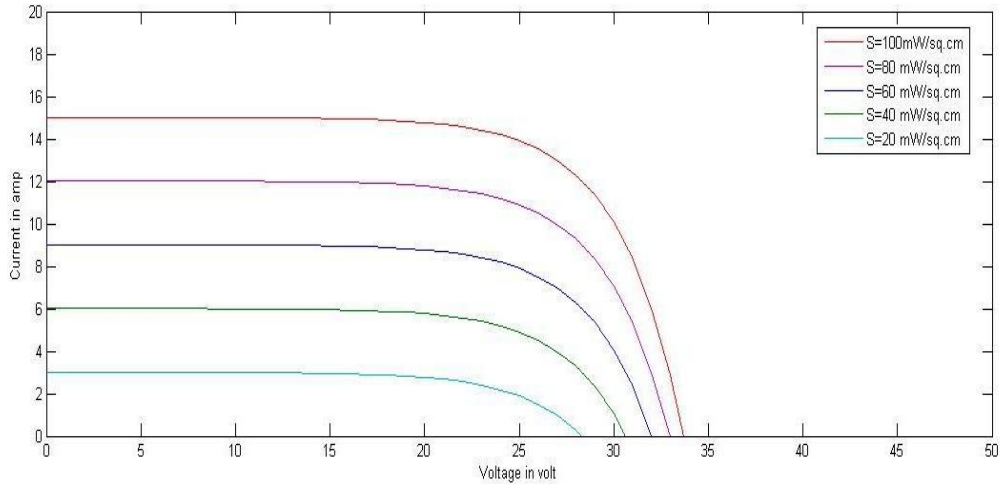


Figure 6.1: I-V Curve obtained for 28°C for various irradiance levels.

From Figure (6.1), we observed that by increasing the solar radiation at constant temperature the voltage and current output from PV array also increases. Hence at higher insolation we can get our required level voltage.

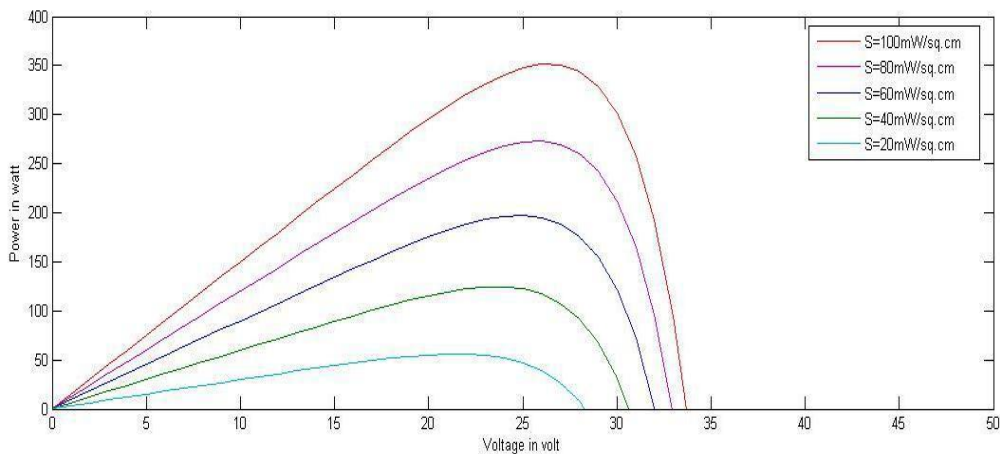


Figure 6.2: P-V Curve obtained for 28°C for various irradiance levels.

From Figure (6.2), we observed that by increasing the solar insolation level, the power output from PV array increases.

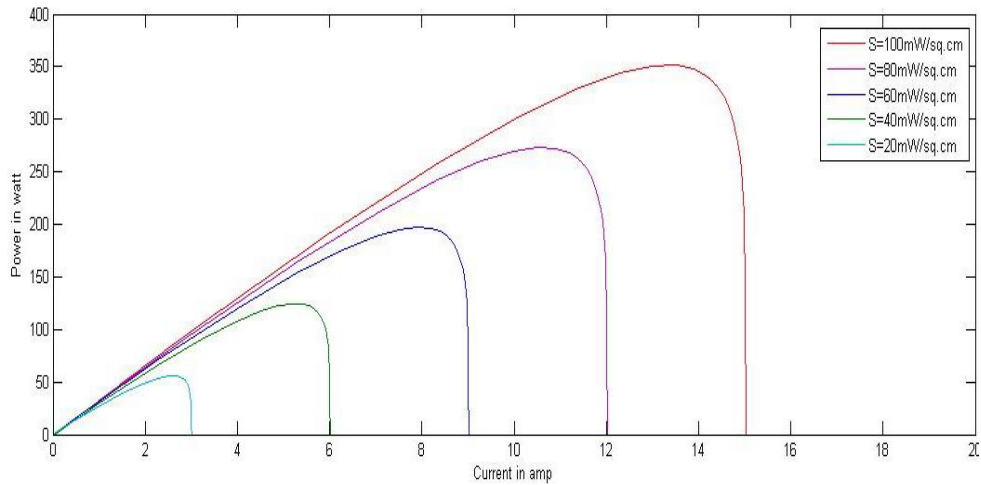


Figure 6.3 P-I curves obtained at 28°C for various irradiance levels.

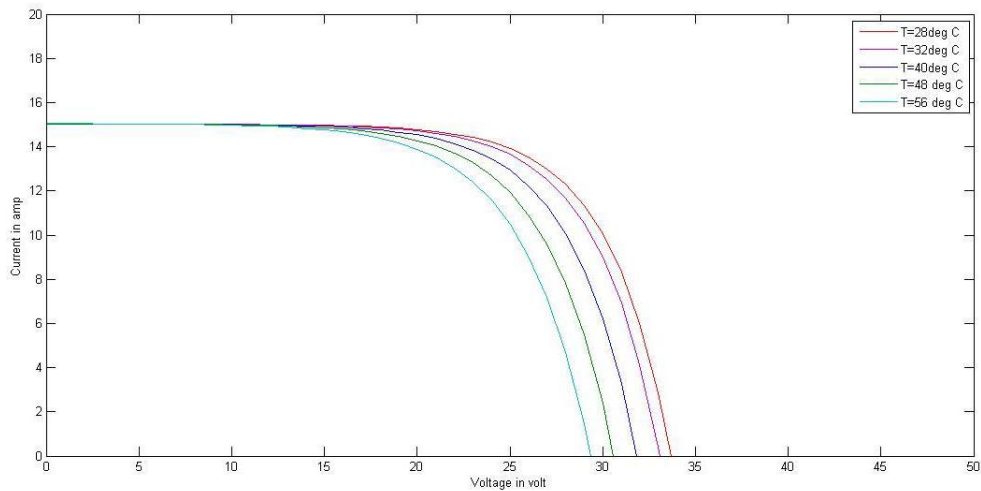


Figure 6.4 I-V curves obtained at an irradiance of 100 mW /cm² for various temperatures.

From Figure (6.4), we observed that by increasing the temperature level at constant irradiance, the voltage output from PV array decreases but current output increases slightly with respect to voltage and, hence the power output from PV array decreases.

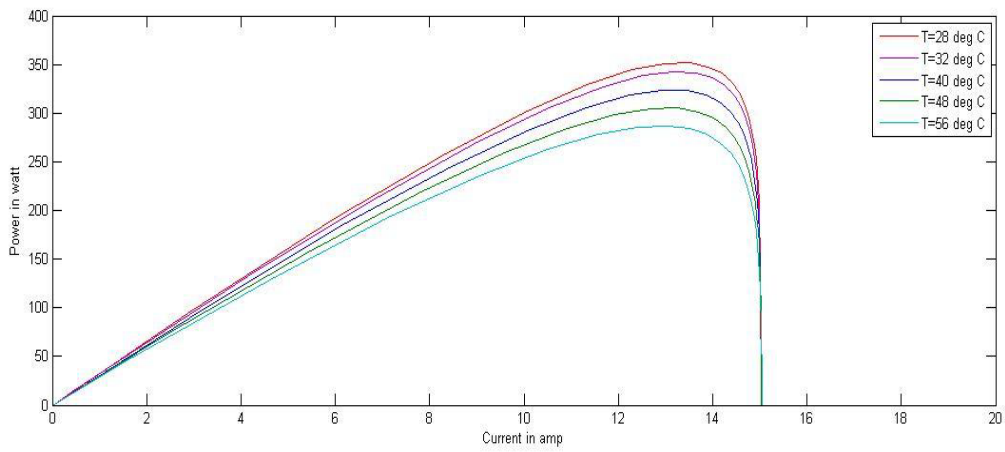


Figure 6.5 P-I curves obtained at an irradiance of 100 mW/cm^2 for various temperatures

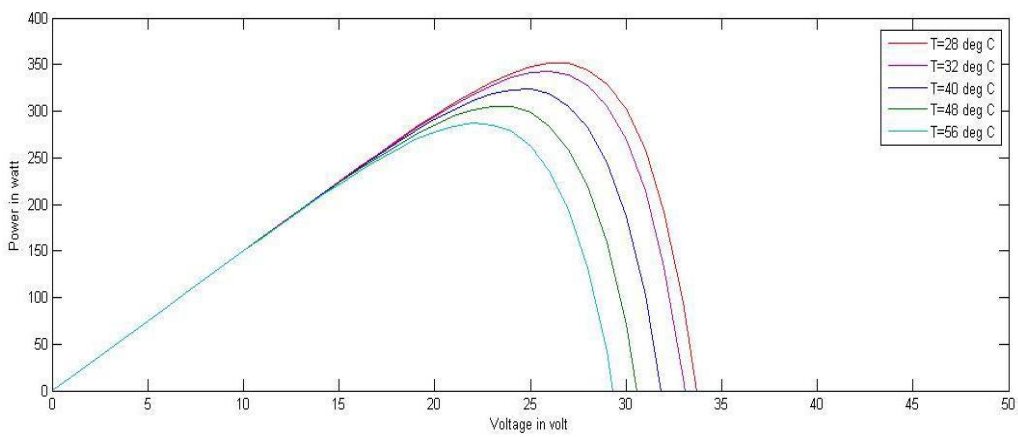


Figure 6.6 P-V curves obtained at an irradiance of 100 mW/cm^2 various temperatures

6.2.1 Parameters used in MATLAB for Converter and Controller

The values of the parameters used in developing the MATLAB code for the converter and PID controller have been tabled below

Table 6.2: Converter and PID Controller Parameters for Simulink

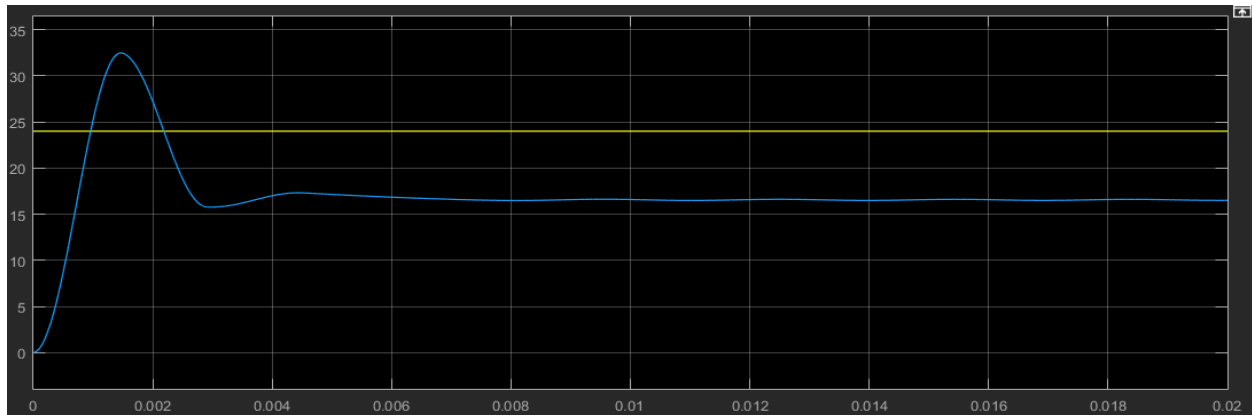
Parameter	Value
Input Voltage	90V-110V
Output Voltage	200V
Rated Power	800W
Duty cycle	0.5
Boost Inductor	400 μ H
Filter Capacitor	100 μ
Resistive Load	50 Ω
K_p	0.0033
K_I	6.43
K_D	0.0027

The equipment values are set according to the availability in the local market. The K_p , K_I , K_D values of the PID controller are set using the Ziegler Nicholes Method explained earlier.

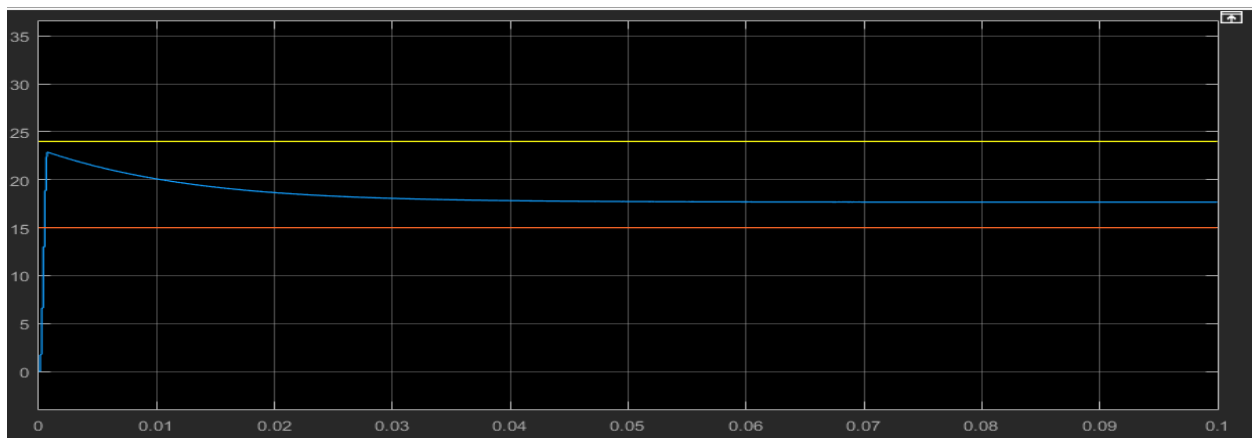
6.2.2 Converter Output

The waveforms obtained from the converters are provided below:

Buck Converter



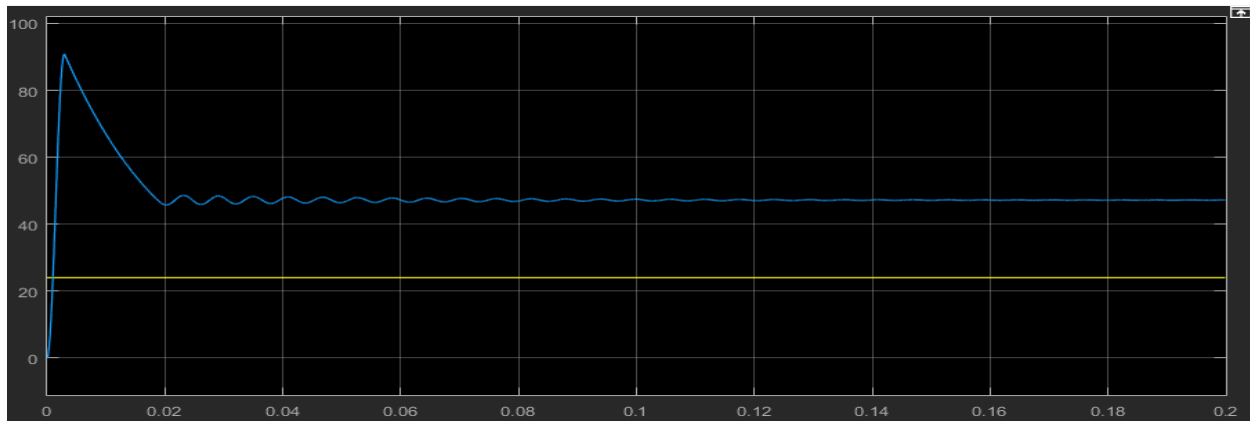
(i)



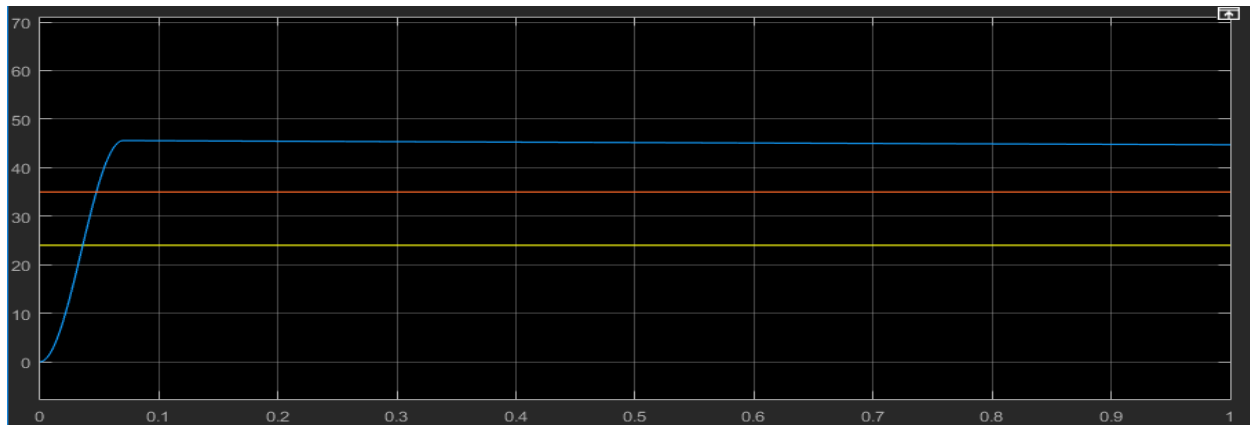
(ii)

Figure 6.7 Input-Output Curves of Buck converter with (i) conventional closed loop and (ii) proposed closed loop with PID

Boost Converter



(i)



(ii)

Figure 6.8 Input-Output Curves of Boost converter with (i) conventional closed loop and (ii) proposed closed loop with PID

As we can see from the comparative study of the output wave shapes, the open loop system has an initial overshoot which was significantly reduced due to the addition of PID controller as a feedback system. It not only improves efficiency of power but also is safe for usage in different appliances.

It also reduced the harmonic distortion compared to the open loop system.

6.2.3 Converter Overshoot Comparison

Buck Converter

Table 6.3: Comparison Between Conventional and Proposed Buck Converter

Proposed Input Voltage, V_i (V)	Conventional closed loop		Proposed closed loop with PID	
	Output Voltage, V_o (V)	Percentage Overshoot (%)	Output Voltage, V_o (V)	Percentage Overshoot (%)
90	28.6	57.63	36.64	3.56
100	34.3	54.27	36.33	2.68
110	39.8	56.37	36.82	3.45

Boost Converter

Table 6.4: Comparison Between Conventional and Proposed Boost Converter

Proposed Input Voltage, V_i (V)	Conventional closed loop		Proposed closed loop with PID	
	Output Voltage, V_o (V)	Percentage Overshoot (%)	Output Voltage, V_o (V)	Percentage Overshoot (%)
90	204.8	52.44	200.8	2.88
100	228.3	51.99	200.6	2.19
110	248.8	53.50	200.4	2.20

Experimental results show that the proposed PID controller when used with Buck and Boost converter provides better output voltage regulation and overshoot reduction, thereby improving the performance of the system.

Chapter 7

Conclusion

The open circuit P-V, P-I, I-V curves we obtained from the simulation of the PV array designed in MATLAB environment explains in detail its dependence on the irradiation levels and temperatures. The entire energy conversion system has been designed in MATLAB-SIMULINK environment. The various values of the voltage and current obtained have been plotted in the open circuit I-V curves of the PV array at insolation levels of 100 mW/cm². The voltage and current values lie on the curve showing that the coupling of the PV array with the boost converter is proper. However, the performance of the photovoltaic device depends on the spectral distribution of the solar radiation.

The proposed Buck & Boost converters with PID controller provides better voltage regulation, overshoot reduction and improves the converter performance compared to the conventional Boost converter. This paper successfully provides a method to satisfy the objective of DC-DC converter to maintain a constant output voltage at the load side. The proposed circuit is simple, easy to understand and can be implemented with no additional components thereby keeping size and cost of manufacturing the converter within considerable range.

References

- [1] Kumar, J. Sai, and Tikeshwar Gajpal. "A Multi Input DC-DC Converter for Renewable Energy Applications." (2016).
- [2] Ortiz, G., J. Biela, D. Bortis, and J. W. Kolar. "1 Megawatt, 20 kHz, isolated, bidirectional 12kV to 1.2 kV DC-DC converter for renewable energy applications." In Power Electronics Conference (IPEC), 2010 International, pp. 3212-3219. IEEE, 2010.
- [3] Li, Wuhua, Xiaodong Lv, Yan Deng, Jun Liu, and Xiangning He. "A review of non-isolated high step-up DC/DC converters in renewable energy applications." In Applied Power Electronics Conference and Exposition, 2009. APEC 2009. Twenty-Fourth Annual IEEE, pp. 364- 369. IEEE, 2009.
- [4] Koutroulis, Eftichios, and Kostas Kalaitzakis. "Design of a maximum power tracking system for wind-energy-conversion applications." IEEE transactions on industrial electronics 53, no. 2 (2006): 486-494.
- [5] Ferdous, S. M., Mohammad Abdul Moin Oninda, Golam Sarowar, Kazi Khairul Islam, and Md Ashraful Hoque. "Non-isolated single stage PFC based LED driver with THD minimization using Cúk converter." In Electrical and Computer Engineering (ICECE), 2016 9th International Conference on, pp. 471-474. IEEE, 2016.
- [6] Yang, Bo, Fred C. Lee, A. J. Zhang, and Guisong Huang. "LLC resonant converter for front end DC/DC conversion." In Applied Power Electronics Conference and Exposition, 2002. APEC 2002. Seventeenth Annual IEEE, vol. 2, pp. 1108-1112. IEEE, 2002.
- [7] Wei, Huai, and Issa Batarseh. "Comparison of basic converter topologies for power factor correction." In Southeastcon'98. Proceedings. IEEE, pp. 348-353. IEEE, 1998.
- [8] Daniele, Matteo, Praveen K. Jain, and Geza Joos. "A single-stage powerfactor-corrected AC/DC converter." IEEE Transactions on Power Electronics 14, no. 6 (1999): 1046-1055.

- [9] Rathi, Ms Kashmira, and Dr MS Ali. "Design and Simulation of PID Controller for Power Electronics Converter Circuits." *International Journal Of Innovative And Emerging Research In Engineering* 3, no. 2 (2016): 26-31.
- [10] Dave, Mitulkumar R., and K. C. Dave. "Analysis of boost converter using pi control algorithms." *International Journal of Engineering Trends and Technology* 3.2 (2012): 71-73.
- [11] R.W. Erickson, D. Maksimovic, and ebrary Inc. (2001). *Fundamentals of power electronics* (2nd ed.). <http://www.springer.com/gp/book/9780792372707>
- [12] B.K. Bose, *Modern power electronics and AC Drives*. Upper Saddle River, NJ: Prentice Hall PTR, 2002.
- [13] S.Busso and P. Mattavelli, *Digital control in power electronics*, 1st ed. San Rafael, Calif: Morgan & Claypool Publishers, 2006.
- [14] D.W. Hart, *Power electronics*. New York: McGraw-Hill, 2011.
- [15] B.W. Kennedy. (2000). *Power quality primer*. Available: <https://www.amazon.com/Power-Quality-Primer-Barry-Kennedy/dp/0071737979>
- [16] N. Mohan, *Power electronics: a first course*. Hoboken, N.J.: Wiley, 2012.
- [17] N. Mohan, T.M. Undeland, and W.P. Robbins. (2003). *Power electronics: converters, applications, and design* (3rd ed.).
- [18] Raviraj, V. S. C., and Paresh C. Sen. "Comparative study of proportional-integral, sliding mode, and fuzzy logic controllers for power converters." *IEEE Transactions on Industry Applications* 33, no. 2 (1997): 518-524.
- [19] Meena, Rajendra. "Simulation study of boost converter with various control techniques." *International Journal of Science and Research (IJSR)* 3, no. 9 (2014): 74-79.
- [20] W. Lu, S. Lang, L. Zhou, H. H. C. Iu and T. Fernando, "Improvement of Stability and Power Factor in PCM Controlled Boost PFC Converter With Hybrid Dynamic Compensation," in *IEEE Transactions on Circuits and Systems I: Regular Papers*, vol. 62, no. 1, pp. 320-328, Jan. 2015.

- [21] Z. Guo, X. Ren, Y. Wu, Z. Zhang and Q. Chen, "A novel simplified variable on-time method for CRM boost PFC converter," 2017 IEEE Applied Power Electronics Conference and Exposition (APEC), Tampa, FL, USA, 2017, pp. 1778-1784.
- [22] T. Meng; H. Ben; Y. Song, "Investigation and Implementation of a Starting and Voltage Spike Suppression Scheme for Three-Phase Isolated Full-Bridge Boost PFC Converter," in IEEE Transactions on Power Electronics, vol.PP, no.99, pp.1-1.
- [23] I. H. Kim and Y. I. Son, "Regulation of a DC/DC Boost Converter Under Parametric Uncertainty and Input Voltage Variation Using Nested Reduced-Order PI Observers," in IEEE Transactions on Industrial Electronics, vol. 64, no. 1, pp. 552-562, Jan. 2017.
- [24] J. Ma, M. Zhu, J. Zhang and X. Cai, "Improved asynchronous voltage regulation strategy of non-inverting Buck-Boost converter for renewable energy integration," 2015 IEEE 2nd International Future Energy Electronics Conference (IFEEC), Taipei, 2015, pp. 1-5.
- [25] A. Singh, A. A. Milani and B. Mirafzal, "Voltage regulation in singlestage boost inverter for stand-alone applications," 2014 IEEE Applied Power Electronics Conference and Exposition - APEC 2014, Fort Worth, TX, 2014, pp. 3011-3016.
- [26] O. Ibrahim, N. Z. Yahaya and N. Saad, "Comparative studies of PID controller tuning methods on a DC-DC boost converter," 2016 6th International Conference on Intelligent and Advanced Systems (ICIAS), Kuala Lumpur, 2016, pp. 1-5.
- [27] L. Mitra and N. Swain, "Closed loop control of solar powered boost converter with PID controller," 2014 IEEE International Conference on Power Electronics, Drives and Energy Systems (PEDES), Mumbai, 2014, pp. 1-5.
- [28] P. Verma, N. Patel, N. K. C. Nair and A. Sikander, "Design of PID controller using cuckoo search algorithm for buck-boost converter of LED driver circuit," 2016 IEEE 2nd Annual Southern Power Electronics Conference (SPEC), Auckland, 2016, pp. 1-4.

- [29] H Atlas, A.M Sharaf, "A photovoltaic Array Simulation Model for Matlab-Simulink GUI Environment", Proce. of IEEE International Conference on Clean Electrical Power, ICCEP 2007, Capri, Italy.
- [30] Jesus Leyva-Ramos, Member, IEEE, and Jorge Alberto Morales-Saldana," A design criteria for the current gain in Current Programmed Regulators", IEEE Transactions on industrial electronics, Vol. 45, No. 4, August 1998.
- [31] K.H. Hussein, I. Muta, T. Hoshino, M. Osakada, "Maximum photovoltaic power tracking: an algorithm for rapidly changing atmospheric conditions", IEE Proc.-Gener. Trans. Distrib., Vol. 142, No. 1, January 1995.
- [32] Mirza Fuad Adnan, Mirza Muntasir Nishat, Mohammad Abdul Moin Oninda. "Design and Simulation of a DC - DC Boost Converter with PID Controller for Enhanced Performance." International Journal of Engineering Research & Technology (IJERT), ISSN: 2278-0181
- [33] W. Xiao, W. G. Dunford, and A. Capel, "A novel modeling method for photovoltaic cells", in Proc. IEEE 35th Annu. Power Electron. Spec. Conf. (PESC), 2004, vol. 3, pp. 1950–1956.
- [34] IEEE Standard Definitions of Terms for Solar Cells, 1969.
- [35] Oliva Mah NSPRI, "Fundamentals of Photovoltaic Materials", National Solar power institute, Inc. 12/21/98.
- [36] Muhammad H. Rashid, "Power Electronics Circuits, Devices and Applications", Third Edition.
- [37] Modelling and Control design for DC-DC converter, Power Management group, AVLSI Lab, IIT-Kharagpur.
- [38] Nielsen, R. 2005, 'Solar Radiation', <http://home.iprimus.com.au/nielsens/>
- [39] www.earthscan.co.uk/Portals/ (Accessed on August 18, 2018)

[40] Application of non-conventional & renewable energy sources, Bureau of Energy Efficiency.

[41] http://en.wikipedia.org/wiki/Solar_power (Accessed on May 24, 2018)

[42] http://en.wikipedia.org/wiki/Photovoltaic_system (Accessed on May 24, 2018)

[43] http://en.wikipedia.org/wiki/Solar_panel (Accessed on May 26, 2018)

[44] <http://www.blueplanet-energy.com/images/solar/PV-cell-module-array.gif/>
(Accessed on May 29, 2018)

[45] http://www.rids-nepal.org/index.php/Solar_Photo_Voltaic.html (Accessed on June 12, 2018)

[46] www.solarhome.ru/img/pv/IV_curve_e.jpg. (Accessed on May 24, 2018)

[47] <http://ecee.colorado.edu/~bart/book/eband5.htm>. (Accessed on May 24, 2018)

[48] [https://en.wikipedia.org/wiki/Overshoot_\(signal\)](https://en.wikipedia.org/wiki/Overshoot_(signal)) (Accessed on November 09, 2018)

Appendix

```
T=28+273;
Tr1=40; % Reference temperature in degree fahrenheit
Tr=((Tr1-32)* )+273; % Reference temperature in kelvin
S=[100 80 60 40 20]; % Solar radiation in mW/sq.cm
%S=70;
ki=0.00023; % in A/K
Iscr=3.75; % SC Current at ref. temp. in A
Irr=0.000021; % in A
k=1.38065*10^(-23); % Boltzmann constant
q=1.6022*10^(-19); % charge of an electron
A=2.15;
Eg(0)=1.166;
alpha=0.473;
beta=636;
Eg=Eg0-(alpha*T*T)/(T+beta)*q; % band gap energy of semiconductor used
cell in joules
Np=4;
Ns=60;
V0=[0:1:300];
for i=1:5
Iph=(Iscr+ki*(T-Tr))*((S(i))/100);
Irs=Irr*((T/Tr)^3)*exp(q*Eg/(k*A))*((1/Tr)-(1/T));
I0=Np*Iph-Np*Irs*(exp(q/(k*T*A)*V0./Ns)-1);
P0 = V0.*I0;

figure(1)
plot(V0,I0);
axis([0 50 0 20]);
xlabel('Voltage in volt');
ylabel('Current in amp');
hold on;

figure(2)
plot(V0,P0);
axis([0 50 0 400]);
xlabel('Voltage in volt');
ylabel('Power in watt');
hold on;

figure(3)
plot(I0,P0);
axis([0 20 0 400]);
xlabel('Current in amp');
ylabel('Power in watt');
hold on;
end
```